mRNA-Activated Matrices Encoding Transcription Factors as Primers of Cell Differentiation in Tissue Engineering

Adriana M. Ledo[a], Ana Senra[b], Héctor Rilo-Alvarez[a], Erea Borrajo[c], Anxo Vidal[c], Maria J. Alonso[a], Marcos Garcia-Fuentes[a,*]

[a] Department of Pharmacology, Pharmacy and Pharmaceutical Technology, IDIS Research Institute, CiMUS Research Institute, University of Santiago de Compostela, 15782 Santiago de Compostela, Spain

[b] Histology Unit, CIMUS Research Institute, University of Santiago de Compostela, 15782 Santiago de Compostela, Spain

[c] Department of Physiology, IDIS Research Institute, CIMUS Research Institute, University of Santiago de Compostela, 15782 Santiago de Compostela, Spain

[*] Corresponding author: marcos.garcia@usc.es

ABSTRACT

Gene-activated matrices (GAMs) encoding pivotal transcription factors (TFs) represent a powerful tool to direct stem cell specification for tissue engineering applications. However, current TF-based GAMs activated with pDNA, are challenged by their low transfection efficiency and delayed transgene expression. Here, we report a GAM technology activated with mRNAs encoding TFs SOX9 (cartilage) and MYOD (muscle). We find that these mRNA-GAMs induce a higher and faster TF expression compared to pDNA-GAMs, especially in the case of RNase resistant mRNA sequences. This potent TF expression was translated into a high synthesis of cartilage- and muscle-specific markers, and ultimately, into successful tissue specification in vitro. Additionally, we show that the expression of tissue-specific markers can be further modulated by altering the properties of the mRNA-GAM environment. These results highlight the value of this GAM technology for priming cell lineage specification, a key centerpiece for future tissue engineering devices.

Key words: GAMs, 3D transfection, mRNA, transcription factors, lineage priming, tissue engineering

Polymer matrices have been largely explored as tissue engineering devices. Since the Food and Drug Administration (FDA) approval of the first collagen-based dermal regeneration template Omnigraft®(1) (Integra Life Sciences, Plainsboro NJ), several material systems have reached the market and paved their way into the clinical setting. Although the first devices largely consisted of biocompatible scaffolds used as fillers or protective patches, polymer matrices soon started to comprise growth factors and other recombinant proteins that help direct the regenerative process. Examples of this successful approach include a rhBMP-7-loaded collagen carrier (OP-1™); a rhBMP-2 loaded collagen sponge (Infuse®); and a sodium carboxymethylcellulose-based gel loaded with rhPDGF (Regranex®)(2). However, these factors are often administered at high doses, to overcome their short half-life, and current formulations offer poor control over their release profiles. This in turn leads to side effects, among which, the risk of malignancies is one of the biggest concerns(3–5).

Trying to overcome these limitations, researchers started to explore the use of gene therapy as an alternative strategy to recombinant protein delivery, and the concept of Gene Activated Matrix (GAM) was described(6). Initially, GAMs were based on plasmid DNA (pDNA), free or complexed to non-viral formulations, encoding the growth factor of interest. This pDNA was loaded within a polymer matrix from which it would be released, transfecting the surrounding cells and inducing the consequent sustained and localized expression of the desired factor(7). Nevertheless, while non-viral delivery of pDNA is preferred over viral vectors due to safety concerns, non-viral formulations are characterized by low gene transfer efficiencies, which hamper their clinical success. This scenario has prompted the development of RNA-based GAMs, based on the superior gene transfer capacity of RNA compared to that of DNA(8). In this regard, different RNA GAMs were explored, ranging from siRNA and miRNA-GAMs(7), to the more recent mRNA-GAMs first described by Elangovan(9). In this work, the authors used chemically modified mRNA encoding the growth factor BMP-2, to study the bone regeneration in rat calvarial defects and demonstrated its superior biocompatibility and regenerative capacity compared to traditional pDNA-GAMs. Subsequent works explored the use of other growth factors and material systems to fabricate mRNA-based GAMs, further consolidating their value(10,11).

Compared to growth factors, transcription factors (TFs) have higher potency and specificity to drive cell reprogramming and directed differentiation(12–16). Realizing their potential for tissue engineering applications, researchers have investigated the use of GAMs encoding pivotal TFs in musculoskeletal development, and established TF-activated GAMs as promising alternatives to “traditional” growth factor-activated GAMs(17,18). Despite this, and the fact that mRNA-encoding TFs can efficiently modulate cell phenotype(16,19–21), to the best of our knowledge, TF-based GAMs have only been explored for pDNA. In this work, we describe a new kind of mRNA-GAMs, activated with lineage-specific TFs and loaded with human mesenchymal stem cells (hMSCs), to direct cell specification in injured or diseased tissues. To this end, fibrin hydrogels were activated with nanocomplexed mRNA encoding SOX9 (cartilage)(22,23) and MYOD (muscle)(24), to promote MSC chondrogenic and myogenic differentiation. Compared to previously explored TF pDNA-GAMs, we hypothesized that the rapid gene modulation induced by mRNA could trigger a faster onset of the differentiation cascades, improving the quality of the regenerated tissue and so providing therapeutic benefits compared to current technologies.

Methods

Cell culture

Human adipose derived Mesenchymal Stem Cells (hMSCs) were acquired from tebu-bio (Le Perray-en-Yvelines, France) and ATCC (Manassas, VA, USA) and cultured in α-MEM (Gibco, Life Technologies, Carlsbad, CA, USA) supplemented with 10% fetal bovine serum (Gibco), 1% penicillin-streptomycin (Gibco) and 10 ng/ml bFGF (Peprotech, Rocky Hill, NJ, USA). Cells were detached from the plates using TrypLE solution (Gibco) and plated at 5000-7500 cells/cm^2. Media was changed every 2-3 days and cells were split at 70-80% confluency.

Plasmid design and mRNA synthesis

Yellow Fluorescent Protein (YFP) and SOX9 mRNAs were in vitro transcribed (IVT) from plasmid templates (**Fig. S1**). To construct the YFP plasmid, the YFP coding sequence (CDS) and a SV40 polyadenylation signal were sequentially digested from a pIRES YFP vector (Clontech, Mountain View, CA, USA) using the XhoI and SmaI sites, and ligated into a pBluescript KS (+) vector (Stratagene, San Diego, CA, USA). Digestion products were separated in agarose gels and purified with the Wizard SV Gel and PCR Clean-up system kit (Promega, Madison, WI, USA) before overnight ligation at room temperature with T4 DNA ligase (Promega). For SOX9 plasmid, the SOX9 CDS, a Kozak consensus sequence and the 3' UTR of the α globin gene(16,25,26) were synthesized and cloned into a pCMVTnT expression vector (Promega, Madison, WI, USA) by Genewiz (South Plainfield, NJ, USA). Both plasmids were sequence-verified (Stab Vida, Caparica, Portugal) and DH5α *E. Coli* bacteria were transformed for their propagation. Plasmids were extracted from the bacterial cultures and purified with the NucleoSpin Plasmid Kit (Macherey-Nagel, Dueren, Germany) according to the manufacturer's instructions. Corresponding mRNA sequences were synthesized with the Anti-Reverse Cap Analog (ARCA) technology, using the mMESSAGE mMACHINE T7 Ultra kit (Ambion, Foster City, CA, USA) following the manufacturer's protocol. Briefly, plasmids were linearized using XhoI and BamHI restriction enzymes (Promega) and 2-7 enzyme units per μg of pDNA. Endonuclease digestion was confirmed by gel electrophoresis and 1.35 μg of linearized plasmids were used as templates for each 20 μl reaction. mRNAs were purified via phenol-chloroform extraction using Phase Lock 1.5 ml tubes (5 Prime, Hilden, Germany) followed by ethanol precipitation and quantification by Nanodrop (Thermo Fisher Scientific, Waltham, MA, USA). MYOD mRNA was purchased from Stemgent (Cambridge, MA, USA) and used as supplied.

Preparation and characterization of 3DFectIN complexes

For 3D transfection experiments, 50 μl of 3DfectIN® complexes (OZ Biosciences, Marseille, France), in the specified 3DFectIN: DNA/RNA ratios (μl:μg), were prepared in OptiMEM (Gibco) following the manufacturer's instructions. Briefly, a solution containing 1 μg of mRNA/pDNA was added over a solution containing 1, 2, 3 or 4 μl of 3DFectIN® reagent in a 1/1 v/v ratio, mixed by pipetting up-down and incubated for 20 min at room temperature. Particle mean size and polydispersity index were analyzed by Dynamic Light Scattering (Nanosizer ZS®, Malvern, Worcestershire, UK) without further dilution. Distribution of the complexes within the hydrogels was assessed by fluorescence microscopy (Olympus IX51 operated with a U-RFL-T lamp) after the encapsulation of SYBR®Gold-labeled pDNA complexes. To this end, an aqueous solution of pDNA was labeled by mixing with a 50X DMSO solution of SYBR®Gold Nucleic Acid Gel Stain (Invitrogen) in a ratio 1:1 (μg:μl) and incubated for 5 min at room temperature before complexes were prepared.

Hydrogel preparation and 3D transfection

Human plasma derived fibrinogen and thrombin were purchased from Sigma-Aldrich (St. Louis, MO, USA). Both materials were reconstituted in, Ca^{2+} and Mg^{2+} free, phosphate buffered saline

(PBS) (Invitrogen) at 50 mg/ml and 100 U/ml, respectively, and further diluted with the same buffer before hydrogel formation. Fibrin hydrogels of 2 and 4 mg/ml were prepared using 2.5 U/ml of thrombin and cast in tissue culture plates (Thermo Fisher Scientific). Transfection and characterization assays were performed with 100 µl gels cast in 96 well plates. In differentiation assays, 200 µl gels were cast in 48 well plates. For 100 µl gels, 20 µl of the fibrinogen solution (20 or 40 mg/ml) were added to the bottom of the plate. Then, 10 µl of the cell suspension mixed with 50 µl of OptiMEM (control gels), the cell suspension mixed with 50 µl of 3DFectIN® complexes (gene-activated gels), or 60 µl of OptiMEM (blank gels) were thoroughly blended with fibrinogen by pipetting up-down. After this, 20 µl of the thrombin solution (12.5 U/ml) were quickly mixed with the previous hydrogel blend ($1.5x10^6$ cells/ml of gel) avoiding the formation of bubbles. Plates were placed in the cell incubator at 37°C for 1 h to allow gelation. Finally, 200 µl of culture medium were added on top of each gel. For 200 µl gels, the same procedure was followed but quantities were doubled.

Scanning electron microscopy

Blank and cell-seeded fibrin hydrogels were prepared as previously described (**Hydrogel preparation and 3D transfection**). Blank gels were frozen at -80°C after the gelation process, while hMSCs seeded gels were kept one week in culture before freezing. All gels were freeze-dried in a VirTis Genesis 25 ES freeze-drier (SP Industries, Warminster, PA, USA) under the following program: primary drying at -35°C for 24 h, secondary drying at 0°C for 24 h and 14 h at room temperature. Freeze-dried samples were carefully removed from the plates and metalized with iridium using a Sputer Coater Quorum Q150T-S (Guelph, Ontario, Canada). Samples were visualized in a Zeiss FESEM Ultra Plus with EDX operated at 5 kV.

Cell toxicity and proliferation assays

Toxicity derived from the encapsulation of hMSCs in gene-activated gels was evaluated by MTT assays (Sigma-Aldrich). Cell proliferation was investigated by monitoring the DNA content using the Quant-iT PicoGreen dsDNA assay kit (Invitrogen, Life Technologies, Carlsbad, CA, USA). hMSCs were encapsulated in fibrin hydrogels with or without 3DFectIN® complexes at a density of $1.5x10^5$ and $1.5x10^6$ cells/ml for MTT and PicoGreen assays, respectively. For MTT assays, gels were cultured during 24 and 48 h and PicoGreen assays were run for 12, 24 and 48 h (short assays) or 3, 7 and 10 days (long assays), preserving some gels for day 0 controls. At the desired time points, gels were digested with 100 µl of a 2.5% trypsin solution (30 min, 37**°**C) and transferred to 2 ml tubes. In the case of MTT assays, formazan crystals were solubilized with a 1/1 v/v mix of 20% sodium dodecyl sulfate (SDS) in PBS and isopropanol by vortexing for 15 min at 2000 rpm in an Eppendorf MixMate® (Eppendorf, Hamburg, Germany) followed by absorbance reading (570 nm with 690 wavelength correction) in a Multiskan GO spectrophotometer (Thermo Scientific). The reading values in gene-activated gels were converted to the percentage of the control (non-activated) gels. For proliferation assays, DNA was extracted with a sequential lysis process using an SDS solution (0.1% w/v in PBS) for the first step and a Triton X-100 solution (1% in PBS) for the second step. Samples were vortexed in an Eppendorf MixMate® (15 min at 2000 rpm for each step) to help extraction. Fluorescence readings were performed at 480/520 excitation/emission wavelengths in an EnVision multilabel

plate reader (Perkin Elmer, Whaltam, MA, USA). Blank gels were included to subtract the fluorescence background and calibration was performed against a λ DNA standard.

Hydrogel degradation assay

Cell-mediated degradation of fibrin hydrogels was determined by digesting the gels and measuring the change in protein content over time. Non-activated hydrogels, seeded with hMSCs, were prepared as previously described (**Hydrogel preparation and 3D transfection**) and incubated in culture media at 37°C and 5% CO_2 for 5 days. At day 1, 2 and 5, the media was aspirated, and gels were digested with 100 µl of a 2.5% trypsin solution (30 min, 37**°**C). After digestion, samples were diluted with water and the protein content was quantified as described in **Supplementary information**. Percentage weight change was normalized to day 0.

Chondrogenic differentiation

Chondrogenesis assays were performed in hMSCs below passage 10. For experiments evaluating the kinetics of chondrogenic marker expression, 2 and 4 mg/ml hydrogels were cast in 96 well plates and cultured for 7 and 21 days in Complete Chondrogenic Medium (CCM) consisting of DMEM high-glucose 1 mM pyruvate (Gibco), 100 nM dexamethasone (Sigma-Aldrich), 50 µg/ml ascorbic acid 2-phosphate (Sigma-Aldrich), 40 µg/ml L-proline (Sigma-Aldrich), 1% ITS Premix supplement (Becton Dickinson), 1% penicillin/streptomycin (Gibco) and 10 ng/ml transforming growth factor-β3 (TGF-β3) (Peprotech). Hydrogels (100 µl) were activated with two doses of SOX9 mRNA and pDNA, namely 1 and 0.25 µg per gel, and at desired time points, total RNA was extracted to check for the presence of chondrogenic markers SOX9, aggrecan (ACAN) and collagen type II (COL2A1) by qRT-PCR. For experiments evaluating the quality of the cartilage-like tissue, fibrin hydrogels of 2 mg/ml (0.5 µg mRNA per 200 µl gel) were cast in 48 well plates and cultured in CCM, and CCM without TGF-β3 (Incomplete Chondrogenic Medium, ICM), for 21 days. At the end of the experiments, SOX9-activated gels were retrieved from the plates and the expression of chondrogenic markers was assessed and compared to non-activated gels cultured in the same conditions. Gene expression of SOX9, ACAN, COL2A1 and collagen type X (COLX) was assessed by qRT-PCR. Alcian blue staining and collagen type II immunohistochemistry (IHC) were used to analyze the deposition of extracellular matrix. Media was changed every 3 days in both experiments.

Myogenic differentiation

Two protocols were assayed for myogenic differentiation. For both protocols, fibrin hydrogels of 2 and 4 mg/ml were cast in 48 well plates and cultured for 14 days. In the first protocol, hydrogels were activated with 0.5 µg of MYOD mRNA per gel and cultured in complete growth media for the first day, changing to DMEM high glucose, supplemented with 2% horse serum (Gibco) and 1% penicillin-streptomycin, for the rest of the assay. In the second protocol, hydrogels were activated with 0.25 µg of MYOD and cultured in α-MEM supplemented with 5% fetal bovine serum and 1% penicillin-streptomycin for the first 7 days (growth phase) switching to DMEM high glucose, supplemented with 2% horse serum, 1% penicillin-streptomycin and 10 ng/ml insulin growth factor 1 (IGF-1) (Peprotech), for the rest of the assay (differentiation

phase). At the end of the experiments, hydrogels were retrieved and the expression of myogenic markers was assessed and compared to non-activated gels cultured in the same conditions. Gene expression of myogenic differentiation protein 1 (MYOD), myogenin (MYOG), cadherin 15 (CDH15), myosin heavy chain 2 (MYH2) and myosin heavy chain 3 (MYH3) was evaluated by qRT-PCR whereas myosin IHC was used to analyze myosin protein expression. Media was changed every 2 days in both experiments.

Total RNA extraction

Two hydrogels (100 µl) or one hydrogel (200 µl) per condition were used for RNA extraction. Hydrogels were removed from the plates with the help of a spatula and placed in 1.5 ml tubes. In transfection experiments, gels were washed with 0.5 ml of PBS and centrifuged in an Eppendorf 5430R centrifuge (1500 x g, 5 min, 4°C) to remove any remaining media before the extraction. In the case of chondrogenic differentiation experiments, gels and pellets were washed with PBS, digested with 700 collagenase units (Gibco) for 15 min at 37°C and washed again, before starting the extraction protocol. Centrifugation speed during the washing steps was set at 1500 x g and 100 x g for the gels and pellets, respectively. For each RNA extraction, 350 µl of lysis buffer were used and samples were digested by vortexing for 15 min at 2000 rpm in an Eppendorf MixMate® with the help of two 2.8 mm stainless steel grinding balls (Ops Diagnostics, Lebanon, NJ, USA). Cell lysates were extracted with the SPEEDTOOLS total RNA extraction kit (Biotools, Madrid, Spain) following the manufacturer's instructions. RNA was quantified by UV absorbance using a Nanodrop 2000 spectrophotometer (Thermo Scientific).

cDNA synthesis and qRT-PCR

Reverse transcription was carried out using 100-500 ng of total RNA per sample in a 30 µl final reaction volume. First, total RNA was mixed with random primers and dNTPs (Invitrogen) and kept at 65°C for 5 min. Samples were then incubated with a mix of RNase OUT, 5x first strand buffer and DTT (Invitrogen) for 2 min at 37°C and subsequently placed on ice. Finally, reverse transcriptase (M-MLV, Invitrogen) was included and the cycle was continued as follows: 10 min at 25°C, 50 min at 37°C and 15 min at 70°C. The resulting cDNA (5-30 ng) was used to assemble qRT-PCR reactions in a final volume of 20 µl containing Universal PCR Mastermix and TaqMan assays (Applied Biosystems, **Table S1**). The thermal cycling was done in a StepOne Real Time PCR System (Applied Biosystems) performing a 10 min hold at 95**°**C followed by 40 cycles of 15 sec at 95**°**C and 1 min at 60**°**C. No template controls were used in each reaction as negative control. Gene expression values were normalized to internal controls (β-actin and GAPDH) and presented as a fold change relative to cells plated in 2D before the experiments using the comparative $2^{-\Delta\Delta Ct}$ method(27). In the experiments evaluating SOX9 expression kinetics, the maximum levels of gene expression detected for each condition were arbitrary set as 100% expression. The expression obtained at the other two remaining time points was expressed as a percentage relative to that maximum expression.

Immunohistochemistry

Hydrogels were retrieved from tissue culture plates, washed with PBS and fixed with 10% buffered formalin at room temperature for less than 24 h. After fixation, samples were maintained in 70% ethanol before dehydration and paraffin sectioning. Sections of 4 µm thickness were cut and allowed to adhere to poly-L-lysine treated glass slides overnight at 55 °C. Before staining, sections were dewaxed in xylene and hydrated with graded ethanol. Samples from chondrogenic differentiation experiments were stained for deposited sGAG and collagen content, with Alcian blue (pH 2.5) and Sirius red, respectively. Immunohistochemical staining (IHC) was performed to check for the presence of collagen type II (II-II6B3, DSHB, Iowa City, IA, USA) and myosin heavy chain (clone MY-32 Sigma-Aldrich), after chondrogenic and myogenic differentiation experiments, respectively. Antigen retrieval was performed in Tris-EDTA buffer during 20 min at 95°C in a PT Link (Agilent, Santa Clara, CA, USA). Samples were pre-treated with hydrogen peroxide and blocked with serum free protein block (Dako; Agilent, Santa Clara, CA, USA). Primary antibodies were diluted 1:100 in antibody diluent (Dako) and incubated overnight at 4°C followed by the incubation with goat secondary antibodies labeled with HRP (Dako) at 1:100 for 1 h and the staining with 3,3'-diaminobenzidine (DAB). Negative controls for histology consisted of hydrogels maintained in regular culture conditions. IHC negative controls were obtained by omitting the primary antibodies (**Fig. S2**). All samples were observed using an Olympus BX43 microscope equipped with an Olympus XC50 camera.

Statistical Analysis

The statistical analysis was performed using GraphPad Prism. Where applicable, data are reported as the mean ±SD. Data were compared using One- or Two-way ANOVA and p-values less than 0.05 were considered to be statistically significant.

Results

Synthesis and characterization of gene activated matrices (GAMs)

The main concept of this work was to develop GAMs activated with mRNA coding for transcription factors (TFs) that are master regulators of cell lineage specification: SOX9 (cartilage) and MYOD (muscle). In order to generate these GAMs, mRNA sequences were nanocomplexed with 3DFectIN® and loaded within fibrin-based hydrogels together with human mesenchymal stem cells (hMSCs). The same GAMs, activated with pDNA, were used as a benchmark throughout the study (**Fig. 1A**). In an initial characterization step, GAMs were prepared with polynucleotides encoding the reporter sequence Yellow Fluorescent Protein (YFP), and different 3DfectIN:polynucleotide ratios were evaluated in terms of nanocomplex size, polydispersity index, and payload association efficiency. Increasing 3DfectIN:polynucleotide ratios from 1:1 to 4:1 (µl:µg) produced smaller and less polydisperse mRNA nanocomplexes, whereas pDNA nanocomplexes followed an opposite trend (**Fig. 1B, S3B**). Ratio 1:1 exhibited the best compromise for both polynucleotides regarding particle size and polydispersity index, but this ratio showed an incomplete complexation of the

polynucleotides, that was not observed for the other ratios (**Fig. 1C, S3A**). Consequently, only ratios 2:1 to 4:1 were further used to screen the influence of 3DFectIN:polynucleotide ratios and polynucleotide doses on GAM transfection efficiency. These transfection experiments were performed in U87MG cells and showed that mRNA induced a much higher YFP expression than pDNA, as assessed by fluorescence microscopy (**Fig. S4A**). In addition, cells loaded with either the highest mRNA dose (2 µg) or the highest 3DFectIN:mRNA ratio (4:1) formed clumps and lost their spindle morphology, suggesting that mRNA nanocomplexes loaded with 1 µg mRNA at a 3DFectIN:mRNA ratio of 3:1, provided the best balance between cytotoxicity and transfection efficiency (**Fig. S4A, B**). In order to confirm this result, SOX9 mRNA and pDNA nanocomplexes prepared at 2:1 and 3:1 ratios, were loaded within the matrices and the transgene expression was determined by quantitative real-time polymerase chain reaction (qRT-PCR). As expected, mRNA nanocomplexes prepared at 3:1 ratio showed the higher transfection efficiency (**Fig. S4C**) and hence this ratio was selected for further experiments with hMSCs. Although a 2:1 ratio resulted in pDNA complexes below the micrometric size and effectively encapsulated the payload (**Fig. S3**), a 3:1 ratio was also selected for pDNA complexes, since it was able to transfect as efficiently (**Fig. S4**) and provided a more consistent benchmark for mRNA-activated matrices prepared at a 3:1 ratio.

GAMs prepared at two fibrin concentrations (2 and 4 mg/ml) presented a highly porous and fibrillar micro-architecture (**Fig. 1D**) where the nanocomplexes were homogeneously distributed (**Fig. 1E, S3C**). An increased hydrogel porosity, accompanied by a thicker fibrillar network, was observed in both MSC-seeded gels compared to their blank counterparts, probably due to cell-mediated hydrogel remodeling and matrix deposition. Since hydrogel remodeling is linked to cell-mediated degradation, an experiment was performed to monitor the mass loss of cell-seeded hydrogels over time. Although no significant differences could be observed between both types of matrices after 24 h, the percentage of mass recovery was lower for 2 mg/ml fibrin matrices after 2 and 5 days, indicating their faster degradation (**Fig. 1F**).

Cytotoxicity assays, carried out at 24 h and 48 h, showed no significant impact of the mRNA complexation reagent on hMSC viability regardless of the fibrinogen concentration (**Fig. S5A**). Additionally, DNA quantification assays confirmed that the inclusion of mRNA complexes within the matrices had no significant long-term effect on cell growth compared to control matrices, and that both fibrinogen concentrations induced very similar cell proliferation rates (**Fig. S5B**). Finally, hMSC transfection within mRNA GAMs prepared at 3:1 ratio, was evaluated qualitatively by YFP reporter expression, confirming the results obtained for the model cell line (**Fig. 1G**).

Effect of polynucleotide type and fibrinogen concentration on GAM gene expression

Having confirmed that mRNA-GAMs were able to induce YFP expression in hMSCs, with negligible effects on their viability, we next characterized the influence of the fibrin concentration and the type of polynucleotide (mRNA vs. pDNA) on transfection efficiency. We first sought to determine whether the transfection results observed for SOX9 in the U87MG model cell line (**Fig. S4**), could be reproduced in hMSCs. For this, SOX9 expression in hMSCs entrapped within SOX9-GAMs was quantified by qRT-PCR. In line with the previous results, mRNA-GAMs induced around a two-fold increase in SOX9 expression in hMSCs compared to

pDNA-GAMs. Conversely, no differences in transgene expression levels could be observed between matrices with 2 mg/ml and 4 mg/ml of fibrinogen, independently of whether they were activated with mRNA or pDNA (**Fig. 2A**). Importantly, both GAMs induced a remarkable upregulation (>$5 \cdot 10^4$-fold increases) of SOX9 as compared to control cells, seeded within non-activated matrices. In order to test the effect of RNase resistant mRNA sequences on transfection efficiency, we next performed a set of transfection experiments with MYOD-matrices, activated with methylated MYOD mRNA. As expected, MYOD relative expression, as assessed by qRT-PCR, was very potent in these matrices, achieving levels that were eight orders of magnitude above the controls (**Fig. 2B**). For both SOX9 and MYOD mRNA-GAMs, we verified that the amount of mRNA extracted from the nanocomplexes during sample processing was not enough to contaminate the total RNA extracted from the cells and thus it was not interfering with the qRT-PCR results (**Supplementary methods**, **Fig. S6**).

Gene expression kinetics was mostly determined by the type of polynucleotide, regardless of the matrix concentration. Indeed, despite the variability derived from the use of different stem cell and mRNA batches across the experiments, both SOX9 GAMs showed consistently opposite transgene expression trends: transgene expression levels peaked at early time points for mRNA-activated matrices and at late time points for pDNA-activated matrices (**Fig. 2C**). Interestingly, contrary to the gradual decay in transcription factor expression observed in SOX9-mRNA matrices over time (12-48 h), the MYOD expression induced by MYOD-mRNA matrices was maintained over the entire experiment (48 h) (**Fig. 2D**). Although both SOX9 and MYOD have positive auto-regulation mechanisms(28,29), different rates of these positive feedback loops may result in the different transgene expression levels obtained for both genes. Additionally, the fact that MYOD mRNA was chemically modified to increase its resistance to RNases, compared to the non-modified SOX9 mRNA sequences, may also contribute to the different kinetics of transgene expression.

Chondrogenic differentiation

We next sought to explore whether we could use the differences in gel remodeling and transgene expression kinetics to maximize the expression of tissue differentiation markers. To this end, mRNA- and pDNA-GAMs encoding SOX9 were assayed for chondrogenic differentiation. We first conducted a screening experiment to understand the kinetics of chondrogenic marker expression induced by our devices, and to select the best conditions for further analysis. We tested the two concentrations of fibrin hydrogels (2 and 4 mg/ml) with both types of polynucleotides (pDNA and mRNA) at two different doses (1 and 0.25 µg per 100 µl hydrogel). As a reference standard culture for chondrogenic differentiation, we included high-density cell pellet cultures. Gels and pellets were cultured in Complete Chondrogenic Medium (CCM) for 7 and 21 days and the expression of chondrogenic markers SOX9, aggrecan (ACAN) and collagen type-II (COL2A1), was assessed by qRT-PCR (**Fig. 3**). At day 7, gels activated with 1 µg of pDNA produced the highest SOX9 upregulation followed by gels activated with 1 µg of mRNA. Gels activated with 0.25 µg of both pDNA and mRNA induced a lower SOX9 expression, although their levels were still higher than those of standard cell pellet cultures. The highest ACAN expression at this time point was obtained for both mRNA activated hydrogels, with no

statistical differences between them. Conversely, ACAN levels in pDNA-GAMs and cell pellets were much lower than those corresponding to mRNA-GAMs. Regarding COL2A1 expression, mRNA gels, again, achieved the highest gene expression, followed by pDNA gels and pellet cultures, which showed a very low expression compared to both gels. No statistical differences were found between 2 and 4 mg/ml hydrogels at this time point (7 days) (**Fig. 3, left**). At 21 days, SOX9 expression did not change significantly compared to the expression observed at 7 days, except for the hydrogels activated with 0.25 μg of pDNA, which increased their expression levels by more than five times during this time frame. Differences between 2 and 4 mg/ml matrices were observed at this time point. Indeed, 2 mg/ml matrices induced significantly higher ACAN and COL2A1 expression compared to 4 mg/ml matrices for almost all the conditions tested. Furthermore, despite the variability in COL2A1 levels, most likely related to the use of low amounts of cDNA in the qPCRs due to reduced RNA quantities, detectable COL2A1 cycle threshold values in 4 mg/ml GAMs were only observed when they were activated with 1 μg of mRNA. The concentration of polynucleotides did not have a significant impact on ACAN induction, with similar ACAN levels being achieved for both the high and the low doses. On the contrary, hydrogels activated with 1 μg of mRNA and 0.25 μg of pDNA promoted the highest COL2A1 expression (**Fig. 3, right**). Together, these results show that mRNA-GAMs induce an earlier expression of chondrogenic markers ACAN and COL2A1 than pDNA-GAMs and that this expression is higher in the matrices with the lower fibrin concentration (2 mg/ml).

Having observed that 2 mg/ml GAMs exhibited the highest chondrogenic marker expression and that the lowest SOX9 dose, of 0.25 μg, effectively induced the upregulation of extracellular matrix (ECM)-related genes, we selected these conditions to compare the differentiation of hMSCs encapsulated in SOX9-activated and non-activated matrices. We conducted these induction assays for 21 days in complete and incomplete chondrogenic media (CCM and ICM, with and without TGF-β3), in order to explore the influence of growth factor supplementation on the differentiation outcome. As expected, for both chondrogenic media, SOX9-GAMS resulted in a higher SOX9 gene expression compared to control matrices and reference pellet cultures (**Fig. S7**). Importantly, this upregulation translated into a higher synthesis of chondrogenic markers as observed by qRT-PCR and histological analysis (**Fig. 4A-B**). At the gene level, the upregulation of chondrogenic markers ACAN, COL2A1 and the hypertrophic marker COLX, was only observed for CCM, whereas all GAMs and controls in ICM resulted in their downregulation compared to MSCs at time zero (very high or not detected cycle threshold levels) (**Fig. S7**, **Fig. 4A**). Significant differences among the treatments were found for COL2A1 expression, with mRNA-GAMs inducing two-fold higher levels compared to the other conditions (**Fig. 4A**). In addition, COLX expression was around three orders of magnitude higher in reference pellet cultures compared to all the matrices (**Fig. 4A**). Interestingly, we observed that TGF-β3 supplementation promoted a higher chondrogenic protein expression in mRNA-GAMs (**Fig. 4B left**), whereas the opposite was found for pDNA-GAMs (**Fig. 4B right**). This is likely related to the different SOX9 expression kinetics of both matrices, since the longer SOX9 expression achieved with pDNA-GAMs might be beneficial to sustain the chondrogenic stimuli in the absence of TGF-β3. Indeed, mRNA-GAMs, cultured in CCM, showed an extensive glycosaminoglycan (sGAG) accumulation as assessed by Alcian Blue staining. sGAG deposition was much lower in the rest of the conditions, especially in the case of the reference cell pellet cultures (**Fig. 4B**).

Immunohistochemical analysis revealed similar levels of collagen type-II within both SOX9-GAMs, whereas control matrices did not show appreciable collagen type-II protein expression, and reference pellet cultures exhibited a notably high expression in contrast to their low sGAG secretion. In experiments performed without TGF-β3 supplementation (ICM), collagen type-II mRNA levels were not detected for any of the conditions, but some expression of collagen type-II protein was detected for both GAMs. This protein expression might be related to early time points where SOX9 expression peaks in both GAMs.

Myogenic differentiation

Encouraged by the good results obtained for the chondrogenic differentiation experiments, in a further step, we assessed the potential of MYOD-mRNA matrices for myogenic differentiation. As in the case of SOX9 GAMs, we first conducted a kinetics experiment to evaluate the expression of myogenic markers induced by both types of activated matrices (2 and 4 mg/ml). MYOD matrices were able to induce a high upregulation of MYOD target genes implicated in myogenesis: myogenin (MYOG) expression was upregulated by five orders of magnitude while the integrin cadherin 15 (CDH15) was upregulated by three orders of magnitude (**Fig. 5A**). These upregulations occurred as fast as the induction of MYOD expression (**Fig. 2D**), suggesting the onset of a myogenic differentiation program coinciding with the encapsulation of hMSCs within the matrices. A similar myogenic marker expression trend was observed for both, 2 and 4 mg/ml MYOD matrices, with no significant differences between them.

Next, hMSCs were cultured for 14 days within MYOD-GAMs to perform myogenic differentiation experiments. Two doses and two differentiation protocols were tested in order to maximize the differentiation output. In a first set of experiments, fibrin matrices were activated with 0.5 µg mRNA per 100 µl matrix, and encapsulated hMSCs were cultured in growth medium for one day and in differentiation medium (DMEM high glucose supplemented with 2% horse serum) during the rest of the experiment. In a second set of experiments, matrices were activated with 0.25 µg mRNA per 100 µl matrix and cultured in low serum growth medium (α-MEM supplemented with 5% fetal bovine serum) for 7 days, followed by differentiation medium, supplemented with insulin growth factor 1 (IGF-1), for the next 7 days. At the end of the experiments, gels were retrieved and myogenic marker expression was assessed by qRT-PCR and immunohistochemistry (IHC). In agreement with our previous kinetics experiments, MYOD and MYOG mRNA expression was very high regardless of the differentiation protocol (**Fig. S8A, Fig. 5B**). Interestingly, whereas the mRNA dose directly affected MYOD relative gene expression, with the lower dose yielding 1000 times less expression, MYOG maximum expression was maintained, suggesting that MYOD might be well above its saturation levels for affecting its gene targets such as MYOG (**Fig. S8A, Fig. 5B**). Myosin heavy chain 2 and 3 (MYH2 and MYH3) mRNA expression was also upregulated in both sets of experiments, showing higher expressions for the lower mRNA dose with IGF-1 (**Fig. S8A, Fig.5B**). Compared to MYH2, a marker of adult fast myosin, MYH3 is a marker of muscle regeneration related to incipient muscle differentiation(30), which is probably the reason why it shows a higher variability in the control (non-activated) matrices. Differences between 2 and 4 mg/ml gels were observed in the low mRNA dose/IGF-1

set of experiments. Indeed, while MYOD and MYOG levels in 2 mg/ml GAMs were similar to the ones observed for the high dose experiments, their values were much lower for the 4 mg/ml GAMs (**Fig. S8A**, **Fig. 5B**). Conversely, MYH2 expression was significantly higher in hMSCs encapsulated within 4 mg/ml GAMs (**Fig. 5B**), which translated to a higher myosin heavy chain protein synthesis, as confirmed by IHC (**Fig.5C**).

Discussion

In this work we show that mRNA-activated matrices encoding pivotal transcription factors (TF) in musculoskeletal development, can efficiently direct hMSCs lineage specification for tissue engineering applications. Compared to their pDNA analogs, mRNA-GAMs promoted a 2-fold higher transgene expression, and at least a 50,000-fold increase compared to non-primed cells (**Fig. 2**). This expression was especially potent for RNase resistant mRNA sequences, which is consistent with previous studies performed in 2D(16) and with recently described mRNA GAMs encoding growth factors (GF)(10,11,31). Gene expression kinetics data agreed also with previous 2D experiments, where mRNA transfection induces a rapid transgene upregulation, while pDNA transfection gradually increases over time(16,32). Interestingly, this rapid TF expression kinetics in mRNA matrices led to an earlier onset of the specific cell differentiation programs. Indeed, compared to SOX9 pDNA-GAMs, SOX9 mRNA-GAMs induced a much earlier mRNA upregulation of chondrogenic markers, an effect that was already evident at day 7 after hMSCs encapsulation (**Fig. 3**). MYOD mRNA GAMs further supported this rapid induction of tissue-specific markers, by promoting the upregulation of myogenic markers as early as 12 h after hMSCs encapsulation, even in the absence of myogenic induction media (**Fig. 5**). Importantly, this potent tissue marker expression was translated into the generation of cartilage-like and muscle-like tissues of improved quality. Together, these results suggest that the fast TF upregulation induced by mRNA GAMs, results in a rapid onset of cell differentiation that may be beneficial for tissue regeneration. This might have implications for the clinical translation of GAM-based technologies, especially in sports-related injuries.

Our results also bring insights on the significance of mRNA dose to induce TF-driven differentiation and suggest that, in contrast to the general perception, maintenance of very high TF expression levels as differentiation progresses might be counterproductive. In the case of chondrogenic differentiation, reducing SOX9 mRNA dose by four times, resulted in a dramatic decrease in SOX9 expression, but produced only a slight effect on aggrecan levels, suggesting that there is a plateau in SOX9-induced aggrecan expression (**Fig. 3**). In addition, MSCs cultured within mRNA-GAMs expressed higher levels of collagen-type II than those in pDNA-GAMs, even though those in pDNA-GAMs had higher SOX9 upregulation **(Fig. 4)**. Similarly, halving the mRNA dose resulted in a 1000-times lower MYOD expression, whereas the MYOG maximum expression was maintained (**Fig. 5**, **Fig. S8**). These findings suggest that uncontrolled transcription factor upregulation over prolonged times might block, at least partially, cell phenotype maturation. Previous works have shown that high levels of TFs can exert a negative feedback on target gene expression(33–35). Likewise, Yamanaka et al. have shown that TF induction needs to be stopped during induced pluripotent stem cell reprogramming for the process to be successful(36). In light of these observations, one could anticipate that the TF mRNA dose and pharmacokinetics must be considered as important design parameters for TF mRNA GAMs.

Adding to the mounting evidence for the role of the mechanical properties of material systems on cell specification(37–39), we found that the GAM environment influences MSC chondrogenic and myogenic differentiation. Indeed, despite their similar transfection efficiencies, our results show that 2 mg/ml SOX9-GAMs induce a more potent upregulation of chondrogenic markers compared to 4 mg/ml GAMs (**Fig. 3**). For myogenic differentiation, 2 mg/ml MYOD-GAMs again, generated the higher levels of immature markers, but the higher expression of mature markers (i.e. myosin heavy chain) was obtained with 4 mg/ml MYOD-GAMs (**Fig. 5**). Previous studies have highlighted the importance of matrix remodeling through proteolytic degradation as a critical process for tissue formation(40–43). In line with these works, and considering the results of our matrix degradation experiments (**Fig. 1**), we propose that the higher ECM synthesis observed in 2 mg/ml SOX9 mRNA-GAMs, is probably related to their faster degradation which promotes mesenchymal condensation(44–47). Similarly, given the implication of matrix mechanical properties on myotube striation and alignment(48–52), we suggest that the increased myogenic marker expression observed in 4 mg/ml MYOD GAMs, could be related to a better cell alignment derived from their slower degradation. These results present that GAM mechanics may be tuned to further modulate the cell differentiation induced by TF overexpression.

Overall, this work provides the first evidence of mRNA-activated matrix encoding transcription factors as a new tool for controlling cell differentiation. Our results show several strengths for this technology in tissue engineering: (i) potent and fast induction of specific differentiation programs, (ii) controllable transcription factor expression kinetics that allows the process to proceed in a self-regulated fashion once triggered, (iii) broad applicability to many different tissue engineering problems, (iv) capacity to upregulate pivotal differentiation markers, reaching levels higher than most data reported in the literature. Already in this first approximation, we were able to apply this technology to successfully generate cartilage- and muscle-like tissues as confirmed by gene expression and histological analysis. Based on our results for YFP protein expression (**Fig.1**, **Fig. S4**), we estimate that SOX9 and MYOD are expressed in more than 80% of the cells. In addition, we have identified some of the critical parameters affecting the expression of the more mature differentiation markers aggrecan, collagen type-II and myosin heavy chain, such as mRNA dose and the mechanical properties of the scaffold. Our results provide some first insights on how to modulate these factors in order to improve GAM design, but further studies will be required to better elucidate the influence of these variables and to be able to adapt these devices to their target application.

Conclusions

mRNA-activated fibrin hydrogels encoding pivotal transcription factors (TF) SOX9 and MYOD were developed to direct stem cell specification for tissue engineering applications. When compared to previously explored pDNA-activated matrices encoding TFs, these systems could induce an earlier TF gene expression. This TF upregulation, in turn, promoted an earlier induction of the corresponding cell differentiation programs and the expression of tissue-specific markers. Fibrin-based mRNA-activated matrices are cell compatible and easily injectable, representing a suitable cell-based platform. Modulation of mRNA dose and matrix mechanics could further tune cell differentiation, allowing for the optimization of tissue-specific matrices. Based on these attractive properties, we believe that mRNA-activated matrices encoding TFs are promising

devices that could facilitate the application of cell reprogramming strategies in regenerative medicine.

Conflicts of interest

MGF, AML and AV are co-inventors of patent WO2017191345A1 that covers some of the technology described here. The authors confirm that there has been no significant financial support for this work that could have influenced its outcome.

Acknowledgements

This work has been funded by Ministerio de Economía y Competitividad (MINECO-RETOS, Grant MAT2017-84361-R, Feder Funds), Fundación BBVA 2014-PO0110 and Xunta de Galicia (Grupos de Referencia Competitiva, Feder Funds; Convenio para fomentar a actividade investigadora do persoal investigador finalista nas convocatorias de axudas do ERC no marco da H2020). AML was a recipient of a FPU grant from Ministerio de Economía y Competitividad (FPU12/05528). The authors thank Dr. C. Carneiro for technical support.

Data availability

The raw data required to reproduce these findings are available to download from Mendeley Data. The processed data required to reproduce these findings are available to download from Mendeley Data.

References

1. Yannas I V, Lee E, Orgill DP, Skrabut EM, Murphy GF. Synthesis and characterization of a model extracellular matrix that induces partial regeneration of adult mammalian skin. Proc Natl Acad Sci U S A 1989;86(3):933–7.
2. Lo KW-H, Ulery BD, Ashe KM, Laurencin CT. Studies of bone morphogenetic protein-based surgical repair. Adv Drug Deliv Rev 2012;64(12):1277–91.
3. Kang DG, Hsu WK, Lehman RA. Complications associated with bone morphogenetic protein in the lumbar spine. Orthopedics 2017;40(2):e229–37.
4. Epstein N. Complications due to the use of BMP/INFUSE in spine surgery: The evidence continues to mount. Surg Neurol Int 2013;4(6):343.
5. DeVine J, Dettori J, France J, Brodt E, McGuire R. The use of rhBMP in spine surgery: is there a cancer risk? Evid Based Spine Care J 2012;3(02):35–41.
6. Bonadio J, Smiley E, Patil P, Goldstein S. Localized, direct plasmid gene delivery in vivo: prolonged therapy results in reproducible tissue regeneration. Nat Med 1999;5(7):753–9.
7. Raisin S, Belamie E, Morille M. Non-viral gene activated matrices for mesenchymal stem cells based tissue engineering of bone and cartilage. Biomaterials 2016;104:223–37.
8. Sahin U, Karikó K, Türeci Ö. mRNA-based therapeutics — developing a new class of drugs. Nat Rev Drug Discov 2014;13(10):759–80.
9. Elangovan S, Khorsand B, Do AV, Hong L, Dewerth A, Kormann M, et al. Chemically modified RNA activated matrices enhance bone regeneration. J Control Release 2015;218:22–8.
10. Balmayor ER, Geiger JP, Koch C, Aneja MK, van Griensven M, Rudolph C, et al. Modified mRNA for BMP-2 in combination with biomaterials serves as a transcript-activated matrix for effectively inducing osteogenic pathways in stem cells. Stem Cells Dev 2016;26(1):25–34.
11. Khorsand B, Elangovan S, Hong L, Dewerth A, Kormann MSD, Salem AK. A Comparative study of the bone regenerative effect of chemically modified RNA encoding BMP-2 or BMP-9. AAPS J 2017;19(2):438–46.
12. Makiko Iwafuchi-Doi and Kenneth S. Zaret. Pioneer transcription factors in cell reprogramming. Genes Dev. 2014;28(May):2679–92.
13. Takahashi K, Yamanaka S. A decade of transcription factor-mediated reprogramming to pluripotency. Nat Rev Mol Cell Biol 2016;17(3):183–93.
14. Liang Q Le, Wang XX, Yan XF, Yang LJ, Tang DQ, Li DS. Transcription factor directed differentiation of human embryonic stem cells into the pancreatic endocrine lineage. Cell Res 2008;18:S109–S109.
15. Graf T, Enver T. Forcing cells to change lineages. Nature 2009;462(7273):587–94.
16. Warren L, Manos PD, Ahfeldt T, Loh YH, Li H, Lau F, et al. Highly efficient reprogramming to pluripotency and directed differentiation of human cells with synthetic modified mRNA. Cell Stem Cell 2010;7(5):618–30.
17. Im GI, Kim HJ, Lee JH. Chondrogenesis of adipose stem cells in a porous PLGA scaffold impregnated with plasmid DNA containing SOX trio (SOX-5,-6 and -9) genes. Biomaterials 2011;32(19):4385–92.
18. Umebayashi M, Sumita Y, Kawai Y, Watanabe S, Asahina I. Gene-activated matrix comprised of atelocollagen and plasmid DNA encoding BMP4 or Runx2 promotes rat cranial bone augmentation. Biores Open Access 2015;4(1):164–74.
19. Mandal PK, Rossi DJ. Reprogramming human fibroblasts to pluripotency using modified mRNA. Nat Protoc 2013;8(3):568–82.
20. Guo XR, Wang XL, Li MC, Yuan YH, Chen Y, Zou DD, et al. PDX-1 mRNA-induced reprogramming of mouse pancreas-derived mesenchymal stem cells into insulin-

producing cells in vitro. Clin Exp Med2014;15(4):501–9.
21. Aini H, Itaka K, Fujisawa A, Uchida H, Uchida S, Fukushima S, et al. Messenger RNA delivery of a cartilage-anabolic transcription factor as a disease-modifying strategy for osteoarthritis treatment. Sci Rep 2016;6(November 2015):18743.
22. Dy P, Wang W, Bhattaram P, Wang Q, Wang L, Ballock RT, et al. Sox9 directs hypertrophic maturation and blocks osteoblast differentiation of growth plate chondrocytes. Dev Cell 2012;22(3):597–609.
23. Bi W, Deng JM, Zhang Z, Behringer RR, Crombrugghe B De. Sox9 is required for cartilage formation. Nat Genet 1999;22(may):85–9.
24. Davis RL, Weintraub H, Lassar AB. Expression of a single transfected cDNA converts fibroblasts to myoblasts. Cell 1987;51(6):987–1000.
25. Kozak M. An analysis of 5'-noncoding sequences from 699 vertebrate messenger rNAS. Nucleic Acids Res 1987;15(20):8125–48.
26. Holcik M, Liebhaber S a. Four highly stable eukaryotic mRNAs assemble 3' untranslated region RNA-protein complexes sharing cis and trans components. Proc Natl Acad Sci U S A 1997;94(6):2410–4.
27. Pfaffl MW. A new mathematical model for relative quantification in real-time RT-PCR. Nucleic Acids Res 2001;29(9):45e – 45.
28. Tapscott SJ. The circuitry of a master switch : Myod and the regulation of skeletal muscle gene transcription. Development 2005;132:2685–95.
29. Mead TJ, Wang Q, Bhattaram P, Dy P, Afelik S. A far-upstream (-70 kb) enhancer mediates Sox9 auto-regulation in somatic tissues during development and adult regeneration. Nucleic Acids Res 2013;41(8):4459–69.
30. Schiaffino S, Rossi AC, Smerdu V, Leinwand LA, Reggiani C. Developmental myosins: expression patterns and functional significance. Skelet Muscle 2015;1–14.
31. Elangovan S, Khorsand B, Do AV, Hong L, Dewerth A, Kormann M, et al. Chemically modified RNA activated matrices enhance bone regeneration. J Control Release 2015;218:22–8.
32. Andries O, De Filette M, Rejman J, De Smedt SC, Demeester J, Van Poucke M, et al. Comparison of the gene transfer efficiency of mRNA/GL67 and pDNA/GL67 complexes in respiratory cells. Mol Pharm 2012;9(8):2136–45.
33. Kypriotou M, Fossard-Demoor M, Chadjichristos C, Ghayor C, de Crombrugghe B, Pujol J-P, et al. SOX9 exerts a bifunctional effect on type II collagen gene (COL2A1) expression in chondrocytes depending on the differentiation state. DNA Cell Biol 2003;22(2):119–29.
34. Harada A, Mallappa C, Okada S, Butler JT, Baker SP, Lawrence JB, et al. Spatial re-organization of myogenic regulatory sequences temporally controls gene expression. Nucleic Acids Res 2015;43(4):2008–21.
35. Cho HC, Mallappa C, Hernández-Hernández JM, Rivera-Pérez JA, Imbalzano AN. Contrasting roles for MyoD in organizing structures during embryonic skeletal muscle development. Dev Dyn 2015;244(1):43–55.
36. Takahashi K, Yamanaka S. Induction of pluripotent stem cells from mouse embryonic and adult fibroblast cultures by defined factors. Cell 2006;126(4):663–76.
37. Huebsch N, Arany PR, Mao AS, Shvartsman D, Ali OA, Bencherif SA, et al. Harnessing traction-mediated manipulation of the cell/matrix interface to control stem-cell fate. Nat Mater 2010;9(6):518–26.
38. Chaudhuri O, Gu L, Klumpers D, Darnell M, Bencherif SA, Weaver JC, et al. Hydrogels with tunable stress relaxation regulate stem cell fate and activity. Nat Mater 2015;15(3):326–34.
39. Mao AS, Shin JW, Mooney DJ. Effects of substrate stiffness and cell-cell contact on mesenchymal stem cell differentiation. Biomaterials 2016;98:184–91.
40. Almalki SG, Agrawal DK. Effects of matrix metalloproteinases on the fate of mesenchymal stem cells. Stem Cell Res Ther 2016;1–12.

41. Ahmann KA, Weinbaum JS, Ph D, Johnson SL, Tranquillo RT, Ph D. Fibrin degradation enhances vascular smooth muscle cell proliferation and matrix deposition in fibrin-based tissue constructs fabricated in vitro. Tissue Eng Part A 2010;16(10).
42. Page-McCaw A, Ewald AJ, Werb Z. Matrix metalloproteinases and the regulation of tissue remodelling. Nat Rev Mol Cell Biol 2007;8(3):221–33.
43. Oh J, Takahashi R, Adachi E, Kondo S, Kuratomi S, Alexander DB, et al. Mutations in two matrix metalloproteinase genes , MMP-2 and MT1-MMP , are synthetic lethal in mice. Oncogene 2004;23:5041–8.
44. Ghone N V., Grayson WL. Recapitulation of mesenchymal condensation enhances in vitro chondrogenesis of human mesenchymal stem cells. J Cell Physiol 2012;227(11):3701–8.
45. Ray P, Chapman SC. Cytoskeletal reorganization drives mesenchymal condensation and regulates downstream molecular signaling. PLoS One 2015;10(8):1–24.
46. Bian L, Guvendiren M, Mauck RL, Burdick JA. Hydrogels that mimic developmentally relevant matrix and N-cadherin interactions enhance MSC chondrogenesis. Proc Natl Acad Sci 2013;110(25):10117–22.
47. Cosgrove BD, Mui KL, Driscoll TP, Caliari SR, Mehta KD, Assoian RK, et al. N-cadherin adhesive interactions modulate matrix mechanosensing and fate commitment of mesenchymal stem cells. Nat Mater 2016;15(12):1297–306.
48. Engler AJ, Sen S, Sweeney HL, Discher DE. Matrix elasticity directs stem cell lineage specification. Cell 2006;126(4):677–89.
49. Engler AJ, Griffin MA, Sen S, Bönnemann CG, Sweeney HL, Discher DE. Myotubes differentiate optimally on substrates with tissue-like stiffness: Pathological implications for soft or stiff microenvironments. J Cell Biol 2004;166(6):877–87.
50. Page RL, Malcuit C, Vilner L, Vojtic I, Shaw S, Hedblom E, et al. Restoration of skeletal muscle defects with adult human cells delivered on fibrin microthreads. Tissue Eng Part A 2011;17(21–22):2629–40.
51. Heher P, Maleiner B, Prüller J, Teuschl AH, Kollmitzer J, Monforte X, et al. A novel bioreactor for the generation of highly aligned 3D skeletal muscle-like constructs through orientation of fibrin via application of static strain. Acta Biomater 2015;24:251–65.
52. Chen S, Nakamoto T, Kawazoe N, Chen G. Engineering multi-layered skeletal muscle tissue by using 3D microgrooved collagen scaffolds. Biomaterials 2015;73:23–31.

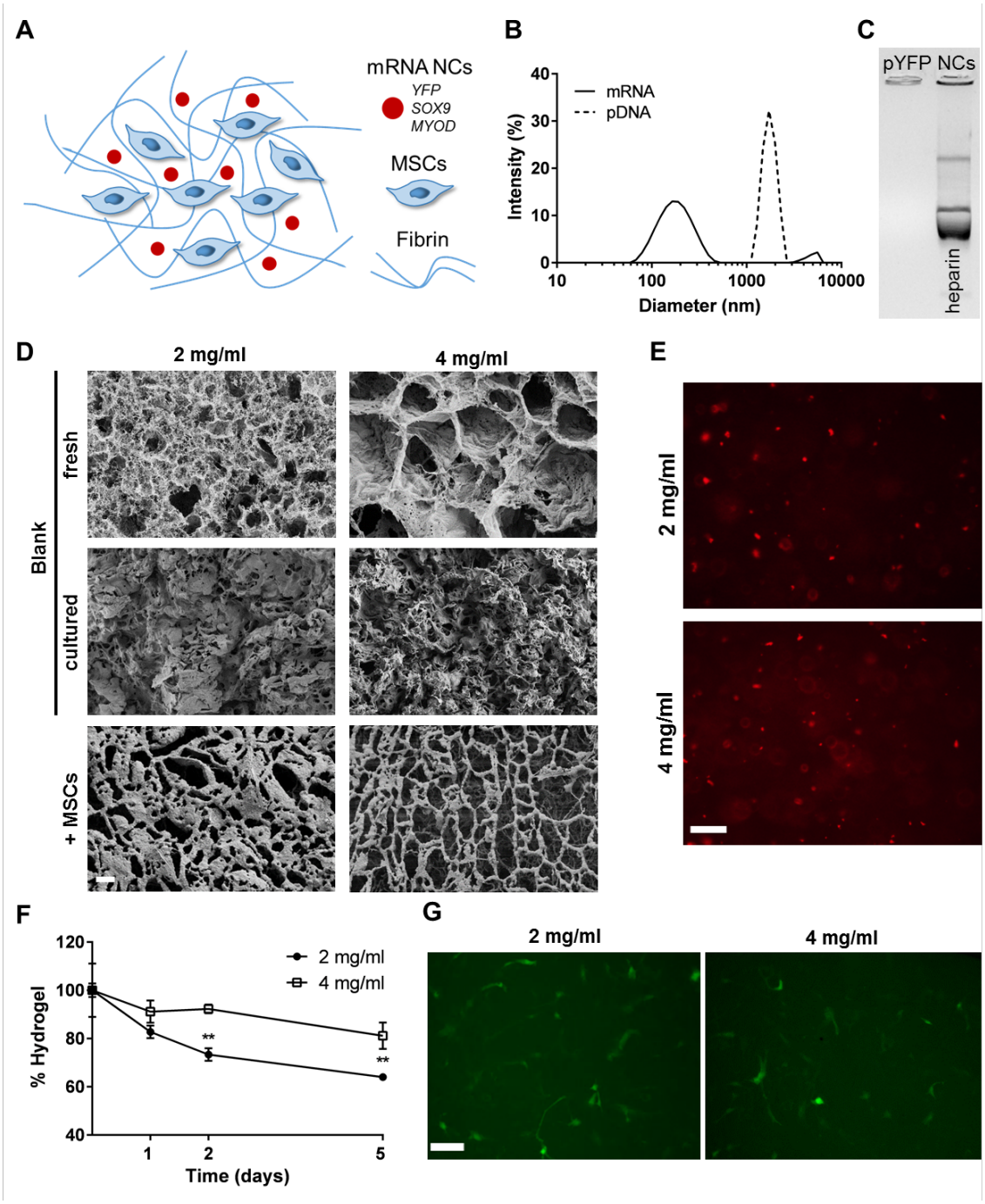
A
mRNA NCs
YFP
SOX9
MYOD
MSCs
Fibrin
B
mRNA
pDNA
Intensity (%)
Diameter (nm)
C
pYFP NCs
heparin
D
2 mg/ml
4 mg/ml
Blank
fresh
cultured
+ MSCs
E
2 mg/ml
4 mg/ml
F
2 mg/ml
4 mg/ml
% Hydrogel
Time (days)
G
2 mg/ml
4 mg/ml

Figure 1

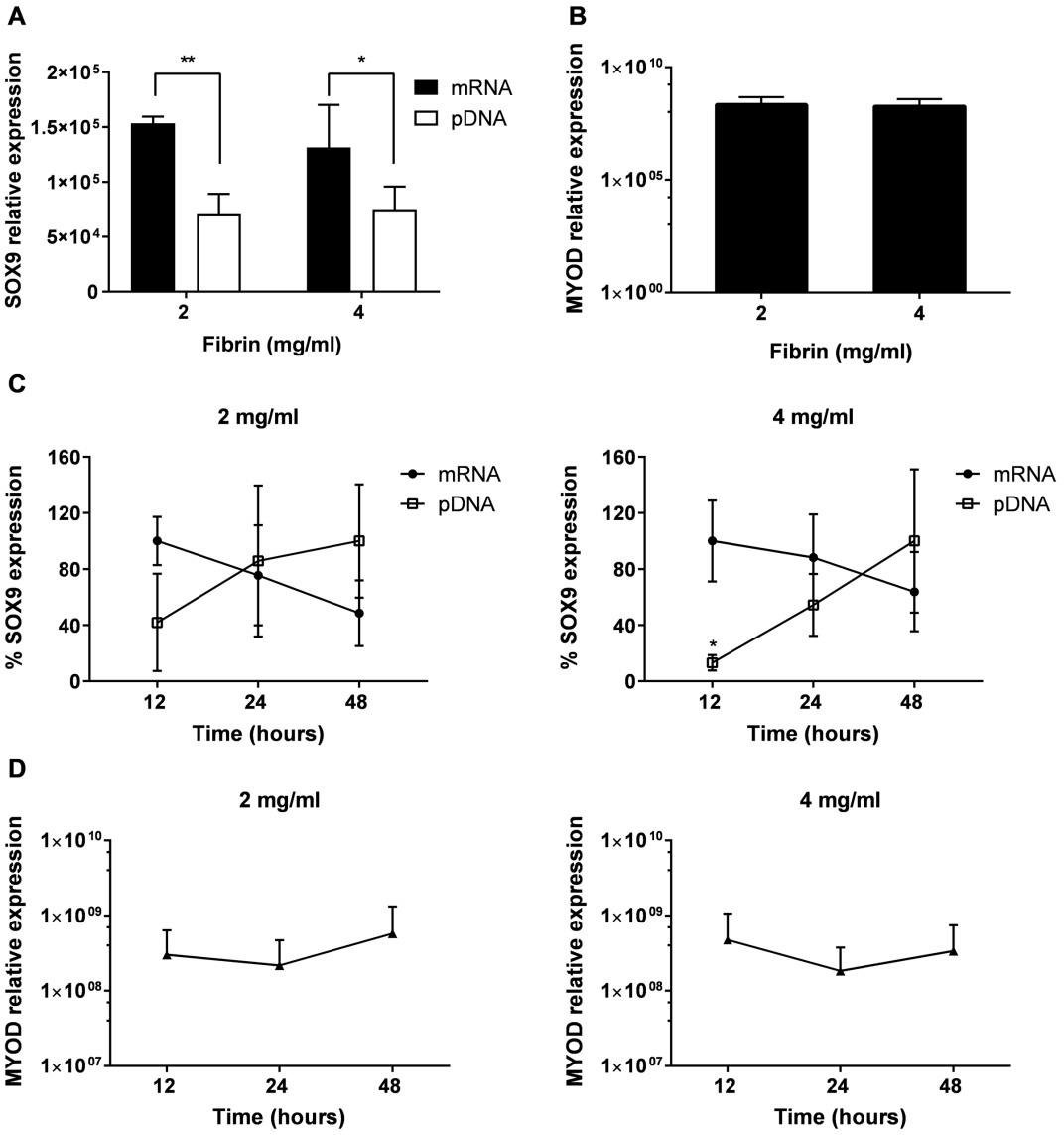
A
SOX9 relative expression
2×10^5
1.5×10^5
1×10^5
5×10^4
0
**
*
mRNA
pDNA
2
4
Fibrin (mg/ml)
B
MYOD relative expression
1×10^10
1×10^05
1×10^00
2
4
Fibrin (mg/ml)
C
2 mg/ml
4 mg/ml
% SOX9 expression
160
120
80
40
0
mRNA
pDNA
*
12
24
48
Time (hours)
D
2 mg/ml
4 mg/ml
MYOD relative expression
1×10^10
1×10^09
1×10^08
1×10^07
12
24
48
Time (hours)

Figure 2

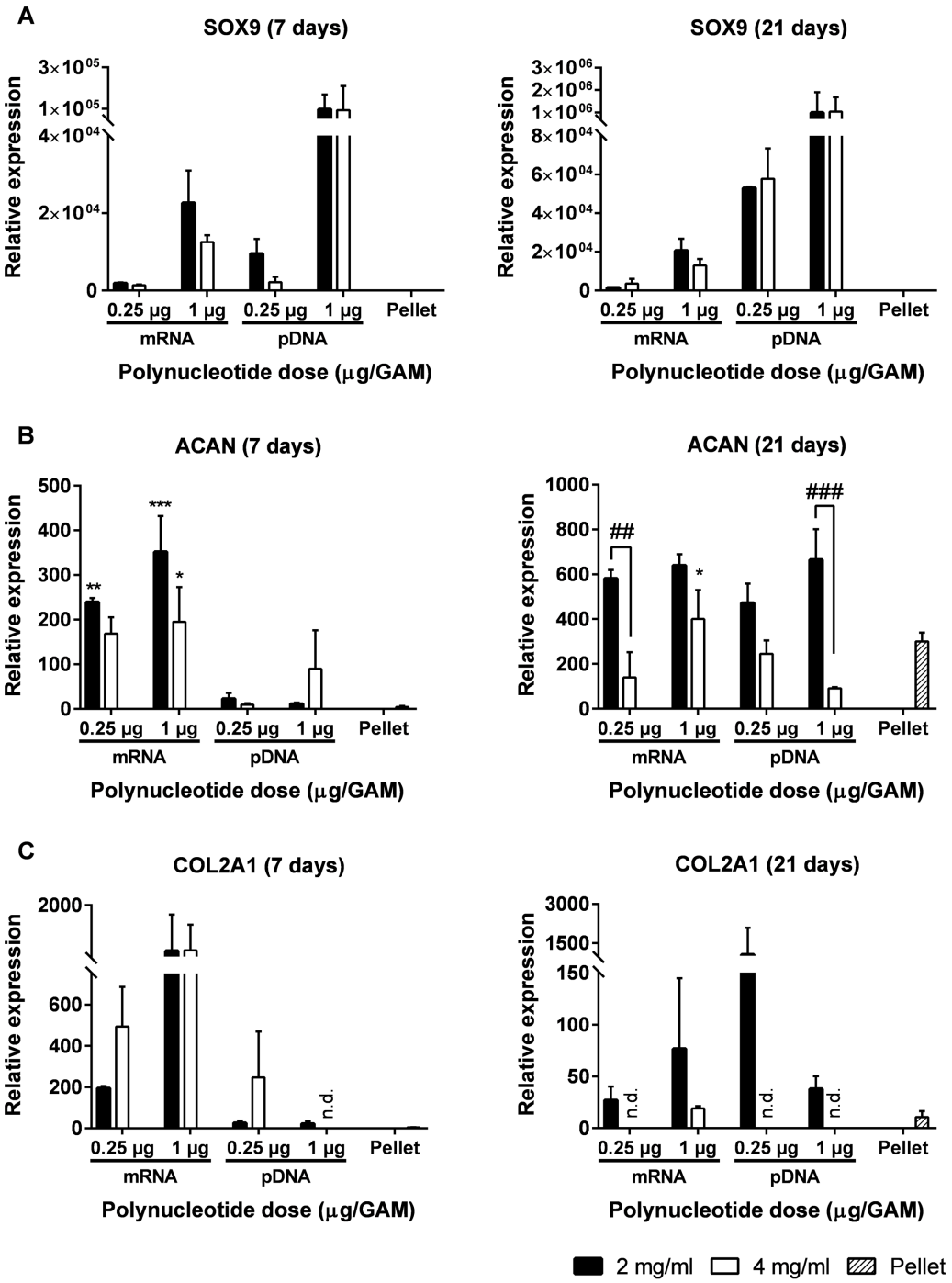
A
SOX9 (7 days)
SOX9 (21 days)
Relative expression
3×10^05
1×10^05
4×10^04
2×10^04
0
3×10^06
2×10^06
1×10^06
8×10^04
6×10^04
4×10^04
2×10^04
0.25 µg
1 µg
Pellet
mRNA
pDNA
Polynucleotide dose (µg/GAM)
B
ACAN (7 days)
ACAN (21 days)
500
400
300
200
100
1000
800
600
**
***
*
##
###
C
COL2A1 (7 days)
COL2A1 (21 days)
2000
3000
1500
150
50
n.d.
2 mg/ml
4 mg/ml
Pellet

Figure 3

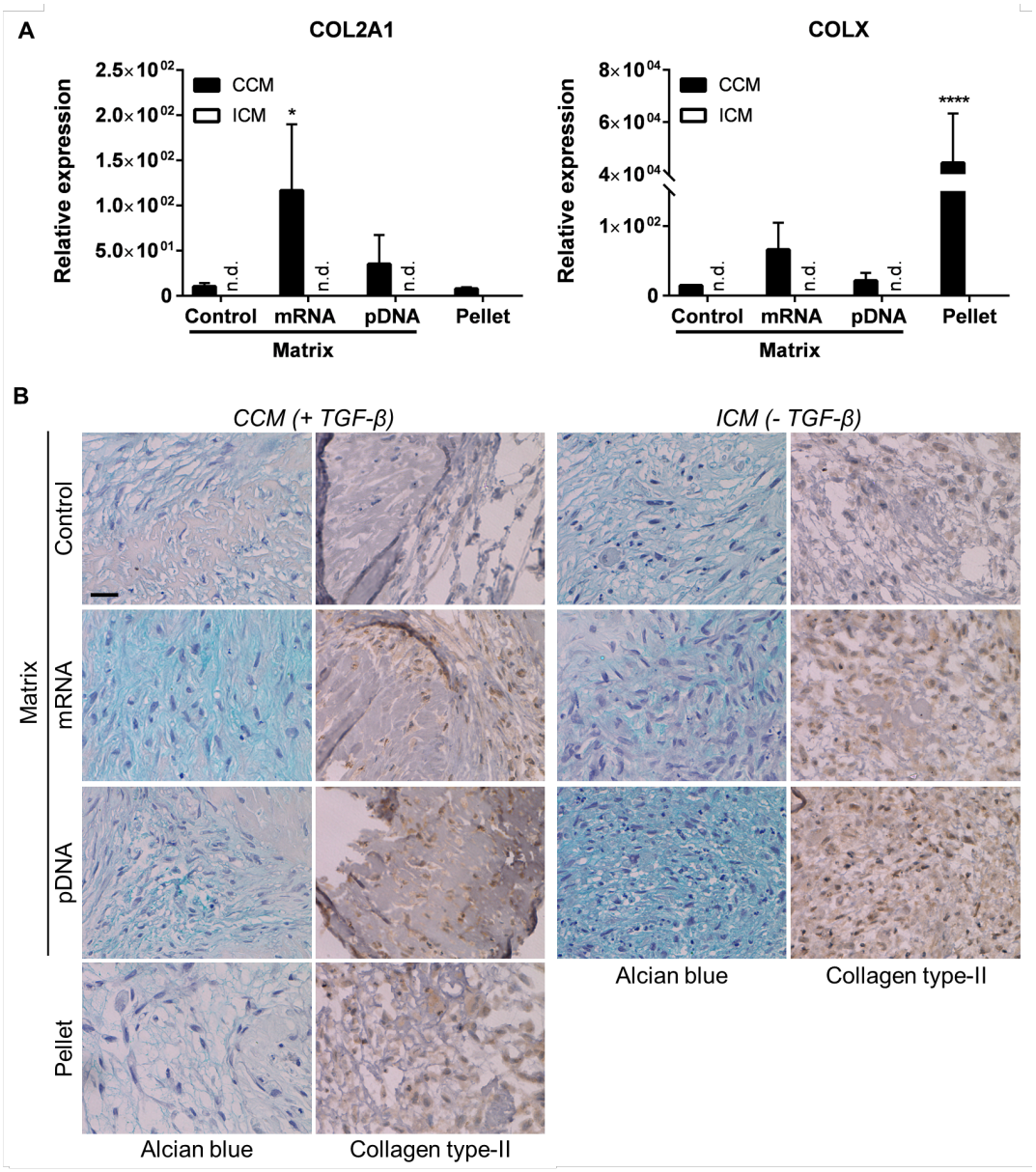
A
COL2A1
COLX
Relative expression
CCM
ICM
*
****
n.d.
Control
mRNA
pDNA
Pellet
Matrix
B
CCM (+ TGF-β)
ICM (- TGF-β)
Control
mRNA
pDNA
Pellet
Matrix
Alcian blue
Collagen type-II

Figure 4

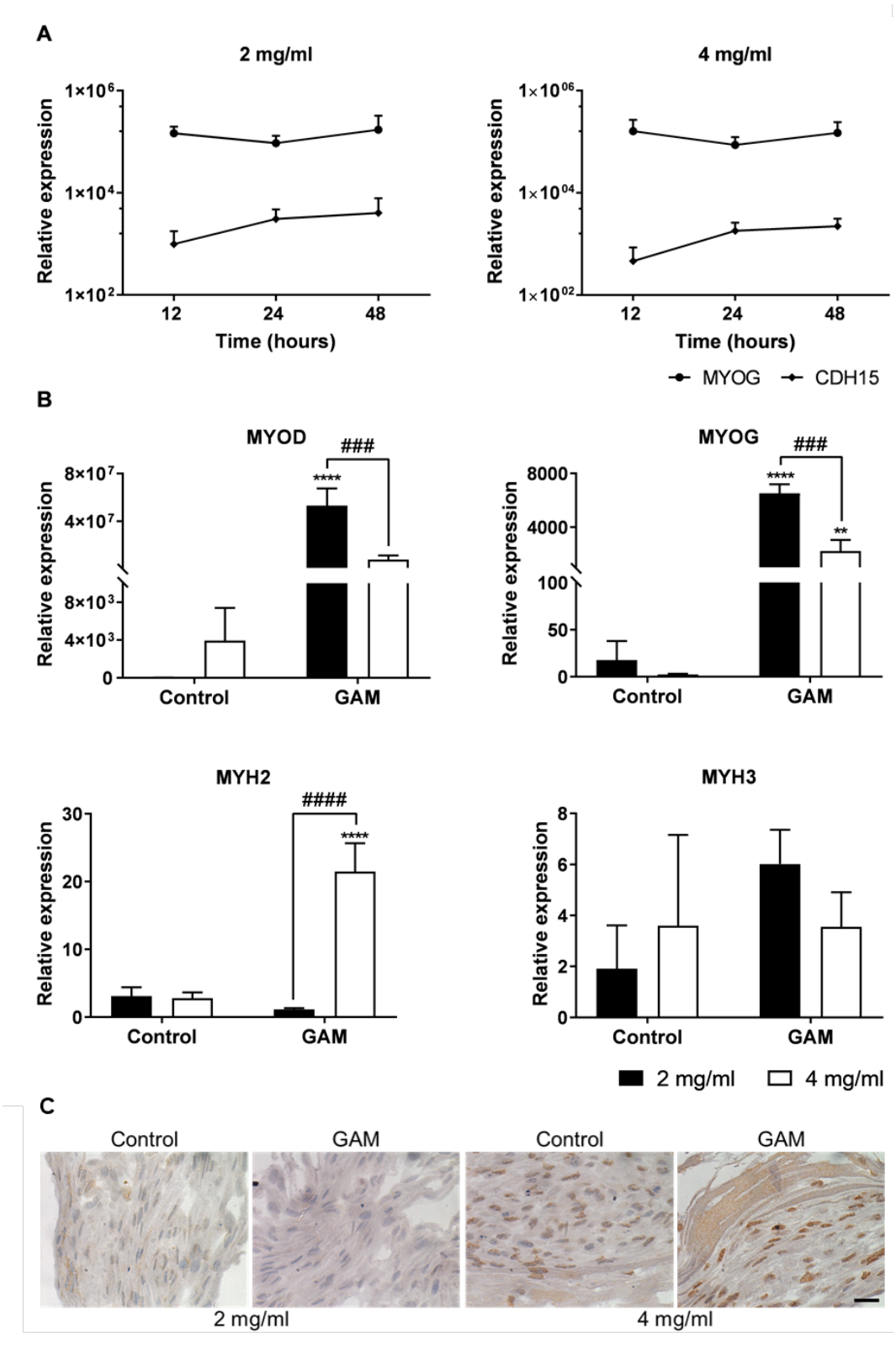
A
2 mg/ml
4 mg/ml
Relative expression
Time (hours)
MYOG
CDH15
B
MYOD
MYOG
MYH2
MYH3
Control
GAM
2 mg/ml
4 mg/ml
C
Control
GAM
2 mg/ml
4 mg/ml

Figure 5

Figure captions

Figure 1. mRNA-GAMs promote stem cell-mediated remodeling and transfection. A) Scheme of the therapeutic concept proposed: human mesenchymal stem cells (MSCs) and mRNA-loaded nanocomplexes (NCs) encoding key transcription factors (TFs) are encapsulated within *in situ* gelling fibrin matrices**.** Transfection occurs when MSCs invade the matrix leading to an enforced TF expression and cell phenotype specification. Objects are not drawn to scale. B) Representative size intensity distribution of mRNA and pDNA 3DFectIN® NCs prepared at 3:1 3DFectIN:polynucleotide ratio (µl:µg) as measured by DLS. C) Gel displacement assay showing the effective association of Yellow Fluorescent Protein (YFP) pDNA to NCs prepared at 3:1 ratio. No pDNA band is detected after loading the NCs in the agarose gel (left lane) unless NCs are previously incubated with heparin to promote pDNA displacement (right lane). D) SEM analysis of the microarchitecture of fibrin matrices immediately after preparation (blank fresh) and after one week in culture with (+MSCs) and without cells (blank cultured). Scale bar = 20 µm for all the images. E) Fluorescence micrographs of SYBR®Gold labelled pDNA NCs (3:1 ratio) loaded into GAMs prepared at two different fibrin concentrations (2 and 4 mg/ml). Scale bar = 50 µm for all the images. F) Degradation rates of 2 and 4 mg/ml fibrin matrices loaded with hMSCs (Two-way ANOVA, n = 3, **P<0.01). Data are shown as mean and standard deviation of three independent experiments at 3:1 3DFectIN:mRNA ratio. G) Representative fluorescence micrographs showing Yellow Fluorescent Protein (YFP) expression in hMSCs 24 h after encapsulation within YPF-activated mRNA-GAMs prepared at 3:1 ratio.

Figure 2. GAM-induced transgene expression is determined by the type of polynucleotide regardless of matrix concentration. A) SOX9 expression 24 h after hMSCs encapsulation within SOX9-activated 2 and 4 mg/ml matrices (Two-way ANOVA, n = 6, *P<0.05, **P<0.01). B) MYOD expression 24 h after hMSCs encapsulation within MYOD-activated 2 and 4 mg/ml matrices (n=4). C) SOX9 expression kinetics of hMSCs encapsulated in 2 mg/ml and 4 mg/ml matrices activated with mRNA and pDNA (n=6). D) MYOD expression kinetics of hMSCs encapsulated in 2 mg/ml and 4 mg/ml matrices activated with RNase resistant mRNA (n=4). Gene expression levels were measured by qRT-PCR, normalized to internal controls (β-actin and GAPDH) and presented as a fold change relative to cells plated in 2D before encapsulation. Maximum levels of transgene expression over the time course shown in C were arbitrary set as 100% for each condition (i. e. time point with maximum expression), and the levels obtained at the other time points were expressed as a percentage relative to this 100%. All experiments were performed at 3:1 3DFectIN:polynucleotide ratio.

Figure 3. SOX9 mRNA-GAMs induce a faster chondrogenic marker expression than pDNA-GAMs. Chondrogenic marker expression of hMSCs encapsulated within 2 and 4 mg/ml mRNA- and pDNA-activated matrices cultured for 7 days (left) and 21 days (right) in complete chondrogenic media. Two doses of mRNA were tested, namely 0.25 and 1 µg per 100 µl gel. Gene expression levels of SOX9 (A), aggrecan (B) and collagen type-II (C) were measured by qRT-PCR, normalized to GAPDH expression and presented as a fold change relative to cells plated in 2D before encapsulation. Not detected cycle thresholds are highlighted as n. d. Data are shown as mean and standard deviation of two replicates in one experiment performed at 3:1 3DFectIN:polynucleotide ratio. A two-way ANOVA was performed to compare gene expression

levels in mRNA and pDNA activated matrices of the same dose and concentration (*P<0.05, **P<0.01, ***P<0.001) and to compare 2 mg/ml and 4 mg/ml matrices with the same dose and genetic material (##P<0.01, ###P<0.001) (n=3). High-density cell pellet cultures are shown as a benchmark for comparison purposes.

Figure 4. SOX9 mRNA- and pDNA-GAMs respond differently to TGF-β3 supplementation. Hydrogels (3:1 3DFectIN:gene ratio) were cultured for 21 days in complete and incomplete chondrogenic media (CCM and ICM, with and without TGF-β3). A) Gene expression levels of collagen type-II (COL2A1) and collagen type-X (COLX) normalized to GAPDH and presented as a fold change relative to cells plated in 2D before encapsulation. Not detected cycle threshold levels are highlighted as n. d. Data are represented as mean and standard deviation bars (n=3) and analyzed by two-way ANOVA (*P≤0.05, ****P≤0.0001). Control designates the control matrices that have the same composition as GAMs but are not loaded with gene nanocomplexes. B) Immunohistological examination of glycosaminoglycan and collagen deposition. Hydrogels were stained with alcian blue for sGAG detection. Collagen type-II was detected by immunohistochemistry. A standard cell pellet culture is shown for comparison. Images are representative of two independent experiments with three replicates per experiment. Scale bar = 20 μm for all the images.

Figure 5. MYOD expression and fibrin matrix concentration jointly promote MSC myogenic maturation in MYOD-GAMs. A) Kinetics of myogenic marker expression myogenin (MYOG) and cadherin 15 (CDH15) in hMSCs cultured in MYOD-matrices (3:1 3DFectIN:mRNA ratio) for 2 days. Cells were maintained in growth media (α-MEM 10% FBS). B-C) Myogenic differentiation experiment. Hydrogels were cultured for 7 days in α-MEM (5% FBS) followed by a 7 days culture in DMEM high glucose (2% HS, 10 ng/ml IGF-1). B) Gene expression levels of myogenic markers MYOD, myogenin (MYOG), myosin heavy chain type 2 (MYH2) and myosin heavy chain type 3 (MYH3) normalized to GAPDH and presented as a fold change relative to cells plated in 2D before encapsulation. Control designates the control matrices that have the same composition as GAMs but are not loaded with gene nanocomplexes. All data are shown as means with standard deviation bars (n=3-6). Two-way ANOVA was performed to compare gene expression levels in control matrices and GAMs (*P<0.05, **P<0.01, ***P<0.001) and in 2 mg/ml and 4 mg/ml matrices (###P<0.001). C) Examination of myosin heavy chain expression by immunohistochemistry. Scale bar = 50 μm for all the images.

SUPPORTING INFORMATION

Supplementary methods

2D Lipofectamine® 2000 transfection

For 2D transfections, cells were plated in 96 well plates approximately 12 h prior to transfection at a density of 90000 (U87MG) or 75000 (hMSCs) cells/cm^2. Four hours before transfection, the media was changed to OptiMEM reduced serum medium (Gibco). Then, 50 µl of Lipofectamine complexes (Gibco), at 0.5:1 Lipofectamine:DNA/RNA ratios (µl:µg), were prepared in OptiMEM following the manufacturer's instructions. Briefly, a solution containing 1 µg of mRNA/pDNA was added over a solution containing 0.5 µl of Lipofectamine® 2000 reagent in a 1/1 v/v ratio, mixed by pipetting up-down and incubated for 20 min at room temperature. Complexes were added over the cells, drop-by-drop, and incubated for 6 hours. Subsequently, complexes were aspirated and cells were maintained in regular growing media until analysis. The transfection reaction was escalated for plates of higher surface areas.

Protein extraction from 2D cultures

Cells were retrieved from the plates, pelleted by centrifugation (5 min, 15°C, 1000 rpm) and washed two times with PBS. RIPA buffer, supplemented with protease inhibitor cocktail (Sigma-Aldrich), was added to the clean pellet (0.5 ml per 60 mm dish) followed by a 20 min incubation on ice. Samples were then sonicated in a Branson Digital Sonifier 250 (30% amplitude, 5 pulses of 1 sec), centrifuged (15 min, 16000xg, 4°C) and supernatants were collected for further analysis. Protein concentration was determined by UV absorbance using a Multiskan GO spectrophotometer (Thermo Scientific) and following the Bradford method. A bovine serum albumin (BSA) calibration curve and the 590/450 nm linearization method[1] were used for quantification.

Western blot

Protein extracts (25-50 µg) were mixed with 5x Laemmli buffer, denatured at 95°C in a Thermoblock for 5 min and separated in 10% PAGE gels. Then, proteins were electroblotted onto a PVDF membrane using a semi-dry blotter (Sigma-Aldrich) operated at 1.2 mA/cm^2 membrane for 1 h. Non-specific binding sites were blocked for 2 hours at room temperature with 5% non-fat milk in 0.05% TNT buffer. The membrane was incubated overnight at 4°C with SOX9 rabbit primary antibody (Santa Cruz Biotechnologies, Dallas, TX, USA) and Tubulin mouse primary antibody (Sigma-Aldrich) using a 1:500 and 1:3000 dilution in 1% TNT, respectively. The membrane was then washed three times with 1% TNT for 10 min and further incubated for 45 min with HRP-conjugated secondary antibodies (GE Healthcare, Chicago, IL, USA), at room temperature and 1:20000 dilution in 0.5% TNT. After three more washes with 0.5% TNT, the immunoblots were finally visualized following the addition of HRP SuperSignal® West Dura Extended Duration Substrate (Thermo Scientific).

Stability of nanocomplexed mRNA and qRT-PCR analysis

SOX9 and MYOD mRNA GAMs (200 µl, without cells) were prepared as described in the methods section "**Hydrogel preparation and 3D transfection**" and incubated in cell culture conditions (MSC growth media, 37°C, 5% CO_2) for 0 h (1 h after hydrogel gelation), 24 h and 7 days (media refreshed every 3 days). At the selected time points, GAMs were retrieved and total RNA was extracted following the methods section "**Total RNA extraction**". At time 0 h, gels were retrieved for RNA extraction before and after RNase digestion. For RNase digestion, 400 µl of RNase A (Thermo Fisher) diluted in growth media were added on top of the GAMs at a final concentration of 1 mg/ml and GAMs were incubated at 37°C for 1 h before RNA extraction. The total RNA extracted was eluted in 30 µl and measured in Nanodrop. The % mRNA recovery for each GAM at the different time points was calculated based on the theoretical amount of mRNA loaded in the GAMs (2 µg in SOX9 GAMs and 0.5 µg in MYOD GAMs). The total RNA obtained at t= 24 h was used to synthesize cDNA and run qRT-PCR reactions. The volume of RNA to template these cDNA reactions was selected based on an average concentration of the total RNA extracted from GAMs loaded with cells and eluted in 30 µl: 72.13 +/- 10.27 ng/µl (mean +/- S.D., n=6). This was made to ensure qRT-PCR reactions were performed in comparable conditions. cDNA (500 ng) was synthesized and qRT-PCR reactions were performed with 10 ng of cDNA per well to detect the cycle thresholds (Cts) of SOX9 and MYOD in the corresponding GAMs according to the protocol described in "**cDNA synthesis and qRT-PCR**". The obtained Ct values were compared to the ones obtained in MSCs in the transfection experiments.

Supporting figures

Table S1. List of TaqMan assays employed for qRT-PCR experiments.

TaqMan assays (Applied Biosystems)	
SOX9 (human)	Hs00165814_m1
ACAN (human)	Hs 00153936_m1
COL2A1 (human)	Hs00264051_m1
COL10A1 (human)	Hs00166657_m1
MYOD1 (human)	Hs00159528_m1
MYOG (human)	Hs01072232_m1
CDH15 (human)	Hs00170504_m1
MYH2 (human)	Hs00430042_m1
MYH3 (human)	Hs01074230_m1
ACT B (human)	Hs99999903_m1
GAPDH (human)	Hs99999905_m1

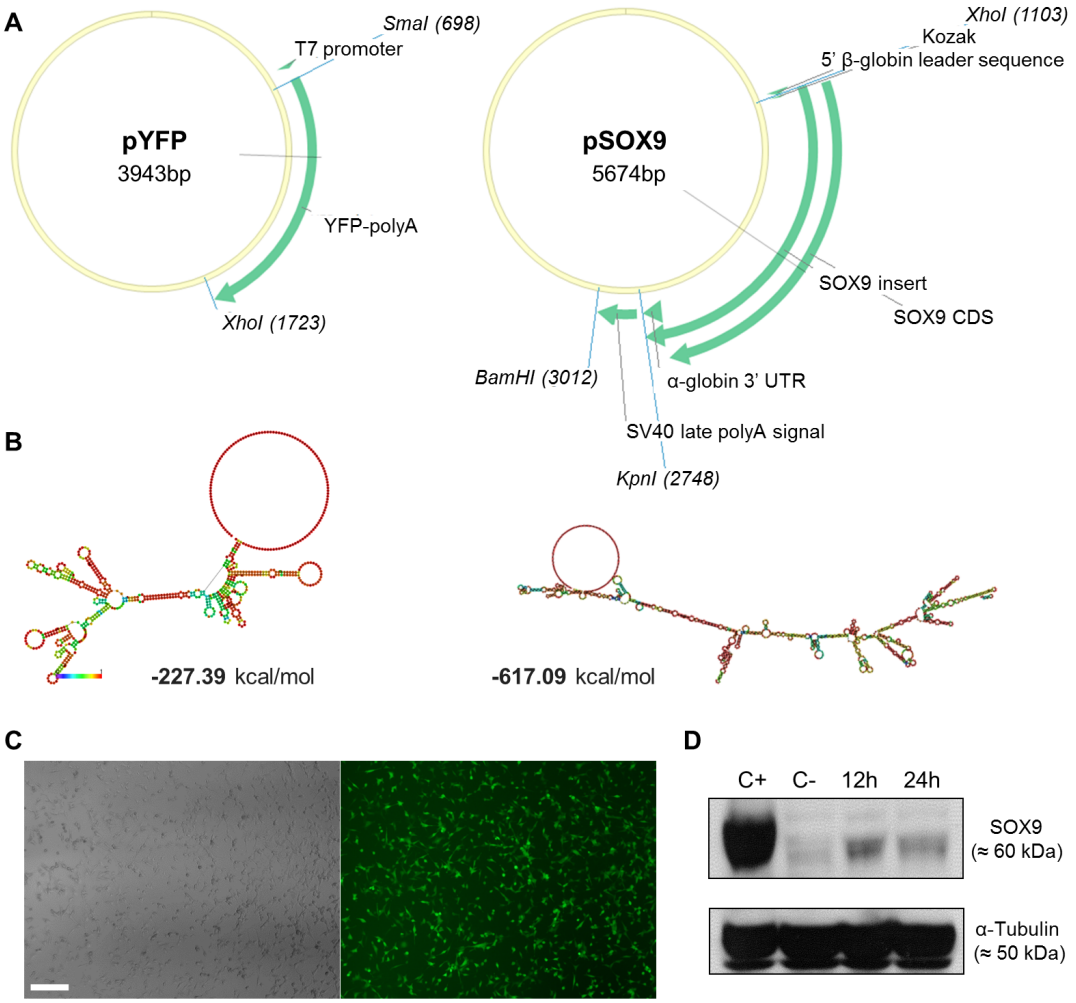

Fig. S1. Plasmid templates and functionality of *in vitro* transcribed mRNAs. A) Maps of YFP (left) and SOX9 (right) plasmids showing the coding sequences (CDS) and relevant restriction sites. B) Minimum Free Energy base pair probabilities according to Vienna RNA website[2] yield a value of -227.39 and -617.09 kcal/mol free energy for the thermodynamic ensemble of YFP and SOX9 RNA molecules, respectively. C) Fluorescent micrograph (right) and corresponding optical micrograph (left) showing YFP protein expression 12 h after YFP mRNA transfection in U87MG cells. Scale bar = 100 µm. D) SOX9 protein expression 12 and 24 h after SOX9 mRNA transfection in HEK293 cells. Protein lysates of untreated and pDNA-transfected cells were used as negative (C-) and positive (C+) controls, respectively.

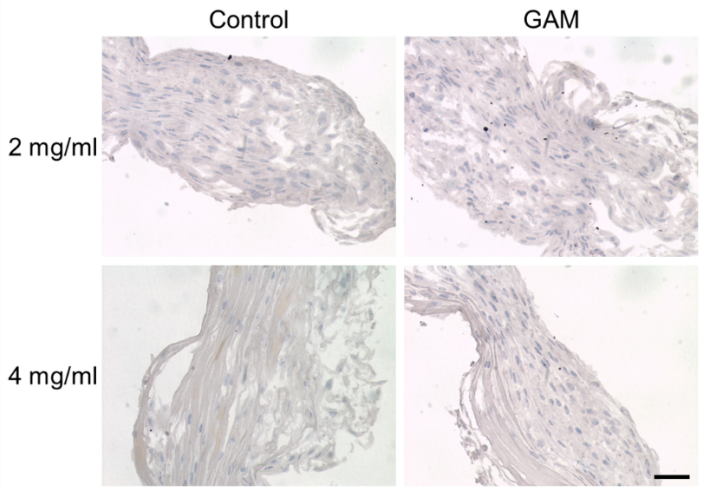

Fig. S2. Negative controls for Myosin Heavy Chain detection by immunohistochemistry. Negative controls were processed in the same way as samples but without the addition of the primary antibody. Controls correspond to the experiment with the two-step schedule: 7 days in α-MEM (5% FBS) followed by a 7 days in DMEM high glucose (2% HS, 10 ng/ml IGF-1). Scale bars = 50 µm for all the images.

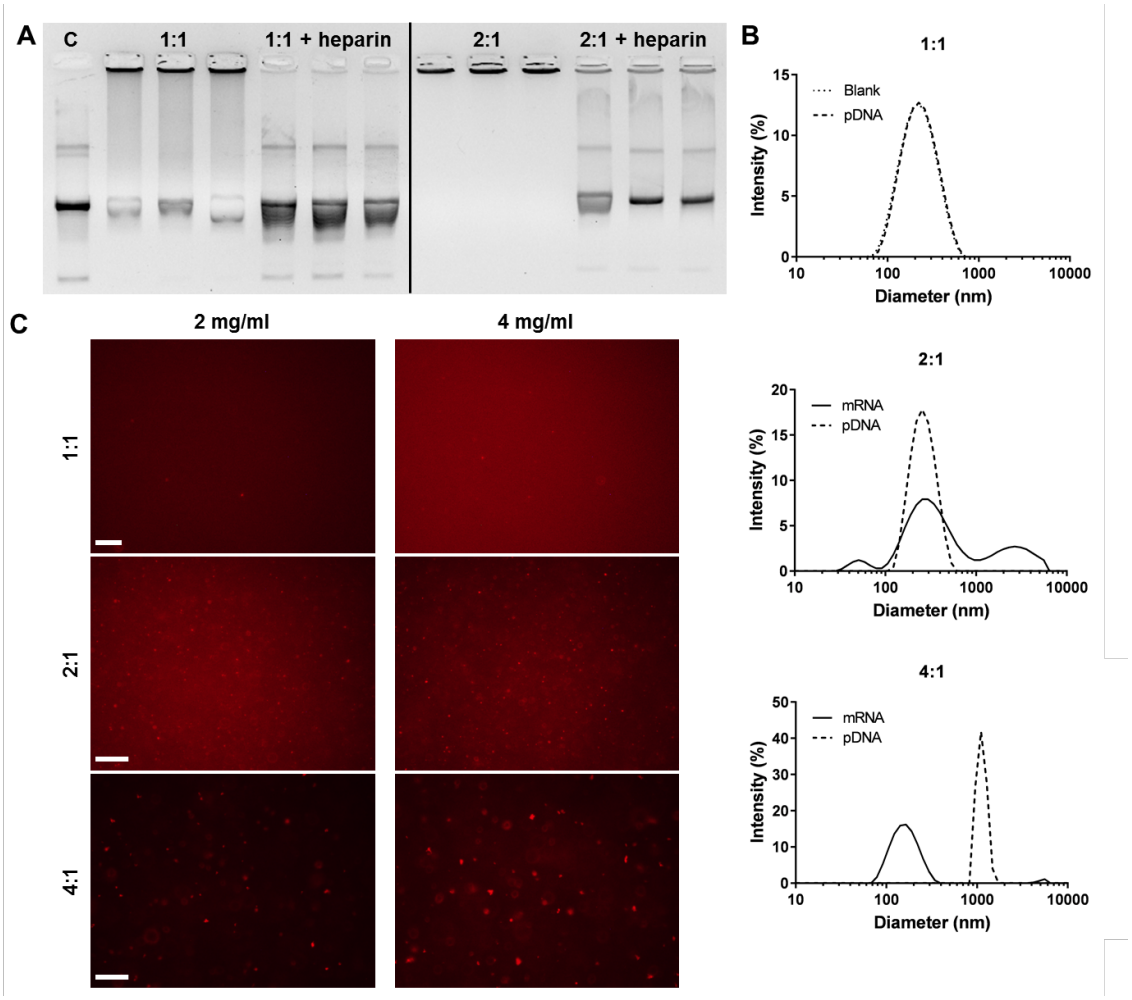

Fig. S3. 3DFectIN: pDNA particles at 1:1 ratio show an incomplete encapsulation of the pDNA cargo. A) Agarose displacement test of 1:1 YFP pDNA-loaded 3DFectIN nanoparticles as compared to 2:1 nanoparticles (µL 3DFectIN:µg pDNA). Naked YFP pDNA is shown as control. B) Representative size intensity distributions of blank (non-loaded) and pDNA-loaded nanoparticles prepared at 1:1 ratio, and mRNA-and pDNA-loaded nanoparticles prepared at 2:1 and 4:1 ratio as measured by DLS. C) Fluorescence micrographs of SYBR®Gold labelled pDNA NPs (1:1, 2:1 and 4:1 ratios) loaded in 2 and 4 mg/ml matrices. Scale bar = 20 µm for 1:1 ratio and 50 µm for 2:1 and 4:1 ratios.

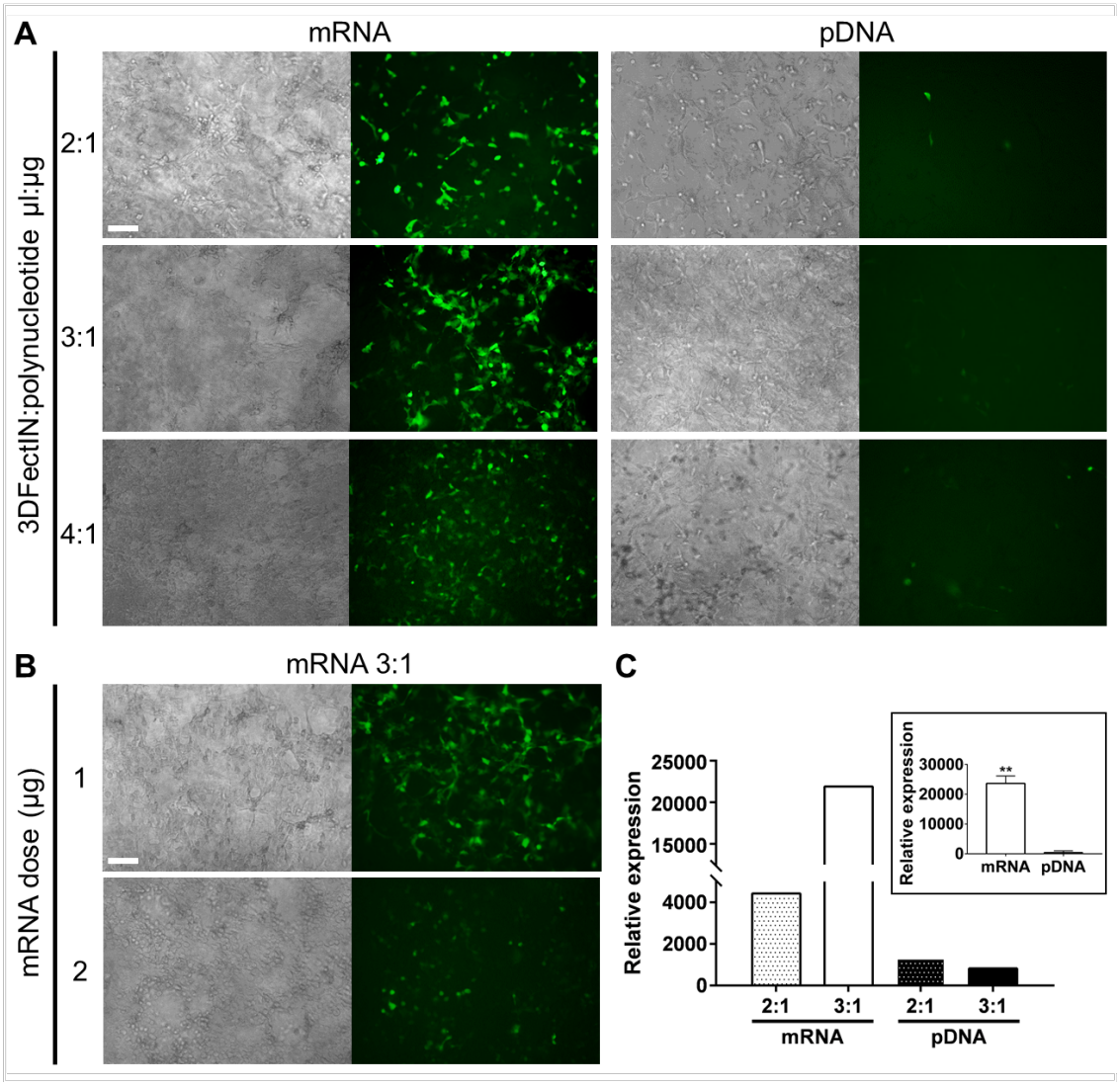

Fig. S4. mRNA nanoparticles prepared at 3:1 ratio exhibit the best compromise between transfection efficiency and cytotoxicity. A) Screening of 3DFectIN:mRNA/pDNA ratios with Yellow Fluorescent Protein reporter sequence and U87MG cell line in 4 mg/mL fibrin gels. Representative fluorescence and optical micrographs corresponding to transfection experiments performed with 1 µg mRNA (left) and pDNA (right) complexed to 3DFectIN® reagent using 2:1 (top), 3:1 (middle) and 4:1 (bottom) 3DFectIN:mRNA/pDNA ratios (µL:µg). Cells became more clumped and lost their spindle morphology at the highest ratio, indicating a higher toxicity. Scale bar = 100 µm for all the images. B) Representative fluorescence and optical micrographs corresponding to transfection experiments performed with 1 and 2 µg of mRNA at 3:1 3DFectIN:mRNA ratio (µL:µg). Cells became more clumped and lost their spindle morphology at the highest dose, indicating a higher toxicity. Scale bar = 100 µm for all the images. C) qRT-PCR transfection screening of U87MG cells cultured within 4 mg/ml fibrin hydrogels comparing mRNA and pDNA nanoparticles prepared at 2:1 and 3:1 ratios. Inset corresponds to nanoparticles prepared at 3:1 ratio (One-way ANOVA, n=2, **P<0.01).

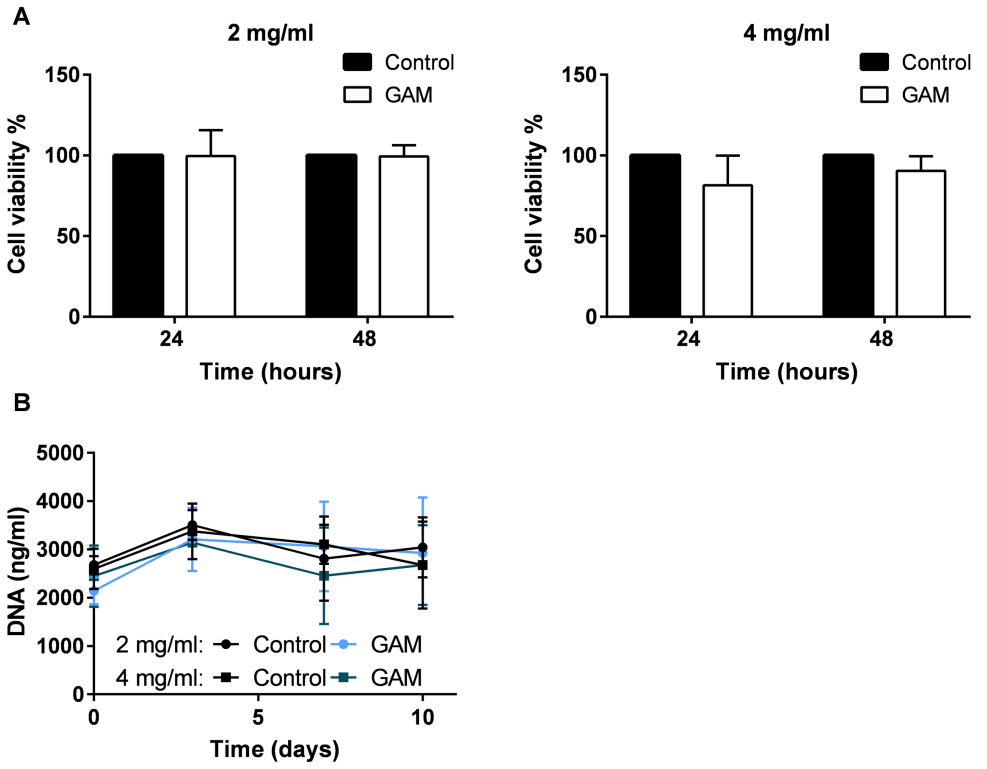

Fig. S5. mRNA-activated fibrin matrices are highly biocompatible. A) MTT cytotoxicity assay 24 and 48 h after the encapsulation hMSCs and 3DFectIN® complexes within 2 and 4 mg/ml gels. B) Ten days proliferation curves for hMSCs in 2 and 4 mg/ml fibrin matrices. Data are shown as mean and standard deviation of three independent experiments at 3:1 3DFectIN:mRNA ratio.

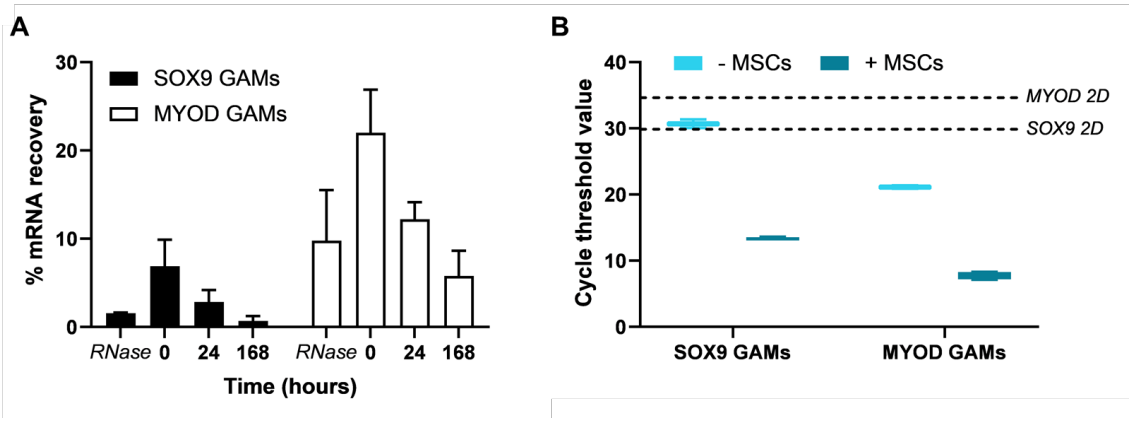

Fig. S6. Stability of nanocomplexed mRNAs within SOX9 and MYOD GAMs. A) % mRNA extracted from SOX9 and MYOD mRNA-GAMs (non-loaded with MSCs) immediately after matrix gelation (time= 0 h) and 24 and 168 h later relative to the theoretical amount of mRNA loaded. GAMs digested with RNase immediately after gelation are shown as reference for mRNA degradation. B) SOX9 and MYOD cycle threshold (Ct) values detected after amplification of the mRNA extracted from SOX9 and MYOD mRNA-GAMs (non-loaded with MSCs), respectively, compared to the levels obtained for the mRNA-GAMs loaded with MSCs. Cts for SOX9 and MYOD detected in MSCs growing in 2D are shown for reference (dashed lines).

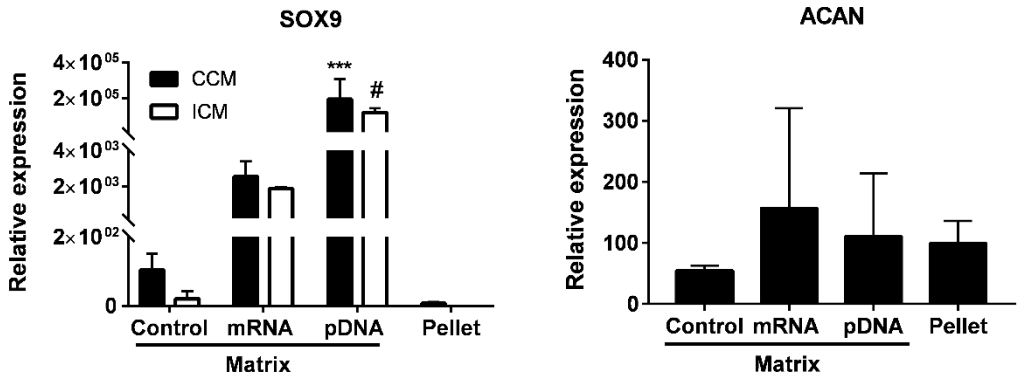

Fig. S7. Expression of chondrogenic markers in hMSCs cultured in fibrin matrices and pellet cultures in complete and incomplete chondrogenic media. Gene expression levels of SOX9 and aggrecan (ACAN) were measured by qRT-PCR, normalized to GAPDH expression and compared to the levels in hMSCs before encapsulation. Data are shown as mean and standard deviation of three replicates in one representative experiment performed at 3:1 3DFectIN:polynucleotide ratio. A two-way ANOVA was performed to compare gene expression levels between CCM and ICM for the same treatment (#P≤0.05) and to compare all treatments within the CCM condition (***P≤0.001) (n=3).

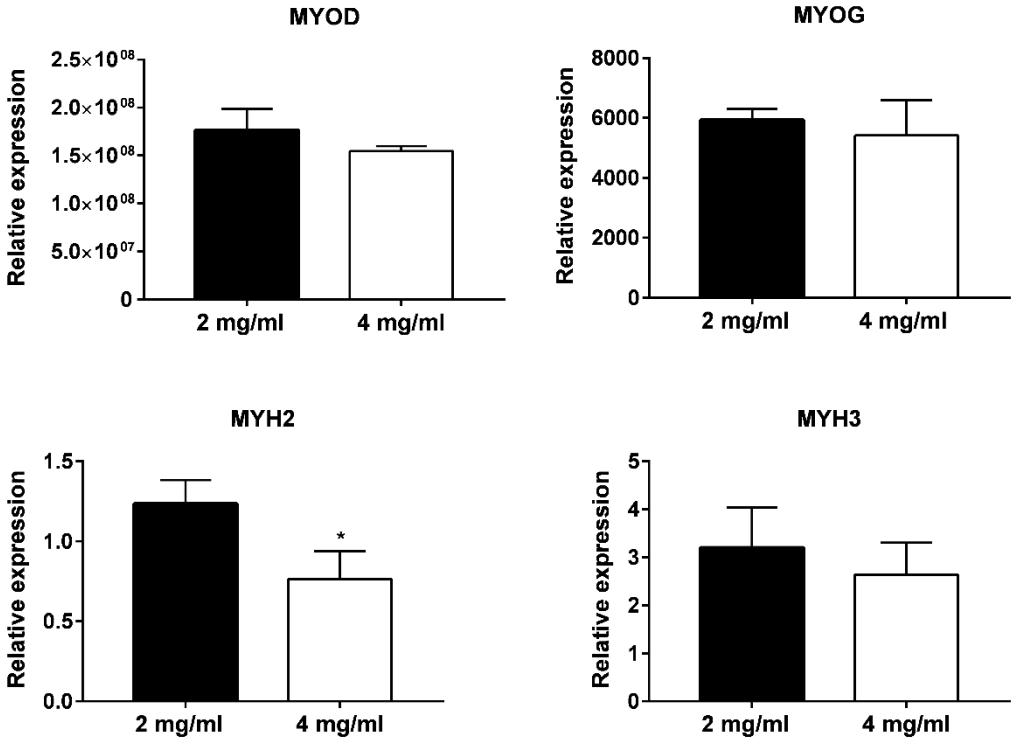

Fig. S8. Myogenic differentiation within MYOD matrices following the differentiation schedule. Hydrogels were cultured for 1 day in α-MEM supplemented with 10% FBS and 13 days in DMEM high glucose supplemented with 2% horse serum. Gene expression levels of myogenic markers MYOD, myogenin (MYOG), myosin heavy chain 2 (MYH2) and myosin heavy chain 3 (MYH3) were measured by qRT-PCR, normalized to β actin expression and compared to the levels in hMSCs before encapsulation. Data are shown as mean and standard deviation of three replicates in one experiment. An unpaired *t*-test was performed to compare gene expression levels (*P<0.05).

References

[1] Zor, T., Selinger, Z. *Anal. Biochem.* **236,** 302 (1996).

[2] Gruber A.R. et al. *Nucleic Acids Res.* **36**(Web Server Issue):W70-74 (2008).